AFRL-ML-TY-TR-2004-4556

Capture of Aerosols by Iodinated Fiber Media

Shanna Ratnesar–Shumate, Prinda Wanakule and **C.Y. Wu**

Department of Environmental Engineering Sciences
University of Florida
412 Black Hall PO BOX 116450
Gainesville, Florida 32611

AIR FORCE RESEARCH LABORATORY
MATERIALS & MANUFACTURING DIRECTORATE
AIRBASE TECHNOLOGIES DIVISION
139 BARNES DRIVE, SUITE 2
TYNDALL AFB, FL 32403-5323

NOTICES

USING GOVERNMENT DRAWINGS, SPECIFICATIONS, OR OTHER DATA INCLUDED IN THIS DOCUMENT FOR ANY PURPOSE OTHER THAN GOVERNMENT PROCUREMENT DOES NOT IN ANY WAY OBLIGATE THE US GOVERNMENT. THE FACT THAT THE GOVERNMENT FORMULATED OR SUPPLIED THE DRAWINGS, SPECIFICATIONS, OR OTHER DATA DOES NOT LICENSE THE HOLDER OR ANY OTHER PERSON OR CORPORATION; OR CONVEY ANY RIGHTS OR PERMISSION TO MANUFACTURE, USE, OR SELL ANY PATENTED INVENTION THAT MAY RELATE TO THEM.

THIS TECHNICAL PAPER HAS BEEN REVIEWED AND IS APPROVED FOR UNLIMITED RELEASE.

JOSEPH D. WANDER, Ph.D
Program Manager

JIMMY L. POLLARD., Colonel, USAF
Chief, Airbase Technologies Division

This report is published in the interest of scientific and technical information exchange and does not constitute approval or disapproval of its ideas or findings.

Do not return copies of this report unless contractual obligations or notice on a specific document requires its return.

REPORT DOCUMENTATION PAGE

Form Approved
OMB No. 0704-0188

1. REPORT DATE *(DD-MM-YYYY)*	2. REPORT TYPE	3. DATES COVERED *(From - To)*
15 Sep 2004	Final Technical Report	Nov 2002–2004

4. TITLE AND SUBTITLE
Aerosol Capture by Iodinated Fiber Media

5a. CONTRACT NUMBER
F08637-02-C-7030

5b. GRANT NUMBER

5c. PROGRAM ELEMENT NUMBER
63384D

6. AUTHOR(S)
Shanna Ratnesar–Shumate, Prinda Wanakule and C.Y. Wu

5d. PROJECT NUMBER

5e. TASK NUMBER

5f. WORK UNIT NUMBER
JON ARMT056W

7. PERFORMING ORGANIZATION NAME(S) AND ADDRESS(ES)
Department of Environmental Engineering Sciences
University of Florida
412 Black Hall, PO Box 116450
Gainesville, FL 32611

8. PERFORMING ORGANIZATION REPORT NUMBER

9. SPONSORING/MONITORING AGENCY NAME(S) AND ADDRESS(ES)
Weapon Systems Logistics Branch
Materials and Manufacturing Directorate, AF Research Lab
139 Barnes Drive, Suite 2
Tyndall AFB, FL 32403-5323

10. SPONSOR/MONITOR'S ACRONYM(S)
AFRL/MLQL

11. SPONSOR/MONITOR'S REPORT NUMBER(S)
AFRL-ML-TY-TR-2004-4556

12. DISTRIBUTION/AVAILABILITY STATEMENT
A---Distribution Unlimited

13. SUPPLEMENTARY NOTES
Technical Monitor: Joe Wander, AFRL/MLQL, 850 283-6240

14. ABSTRACT
Discs of a synthetic fiber medium, before and (in two thicknesses) after coating with finely divided particles of poly(styrene–trimethylammonium iodide) (Triosyn®) resin, were challenged with an aerosol generated by atomizing an aqueous solution of ammonium fluorescein. A six-stage Andersen impactor was used to classify the particles penetrating each of these media and a fiberglass control medium. The coating on each stage was phased between water and methylene chloride to separate the fluorescein from the trapping medium. After application of a correction factor to correct for reaction with iodine, fluorescence of each extract was measured from which physical capture efficiency was calculated for particles within the submicron-to-low-micron range. Capture efficiencies of 97–99% were measured for 1.1–2.1 mm particles at <2 inches of water pressure drop.

15. SUBJECT TERMS
Antimicrobial; aerosol; bioaerosol; filter; fluorescein, iodine; pathogen

16. SECURITY CLASSIFICATION OF:			17. LIMITATION OF ABSTRACT	18. NUMBER OF PAGES	19a. NAME OF RESPONSIBLE PERSON
a. REPORT	b. ABSTRACT	c. THIS PAGE			Joe Wander
U	U	U	UU	56	19b. TELEPHONE NUMBER *(Include area code)* 850 283-6240

EXECUTIVE SUMMARY

A. OBJECTIVE:

The objective of this project was to evaluate the physical capture efficiency of filter media coated with an iodinated resin, which is being considered for possible use in protective gear against biological warfare and bioterrorism.

B. BACKGROUND:

Due to the pathogenic nature of some bioaerosols and recent threats of biological weaponry, methods for effective capture and neutralization of airborne microorganisms are of great interest. A new technology has been developed that combines the use of filtration and iodine disinfection to provide protection against airborne pathogens equal to or better than that afforded by conventional high-efficiency filtration system, and at a lower pressure drop.

C. SCOPE:

The physical capture efficiency of various biocidal media provided by the AFRL was examined at three airflow rates. The capture efficiency as a function of particle size was determined along with the pressure drop associated with each filter.

D. METHODOLOGY:

Ammonium fluorescein particles with a wide size range were generated by atomization and introduced into the biocidal filtration system to be tested. Particles entering and penetrating the filter were classified by particle size using a six-stage Andersen impactor. Both the iodine-treated and blank media were compared to a control with no medium present upstream of the impactor, as well as to a standard glass fiber filter. The captured fluorescent particles were then rehydrated by ammonium hydroxide solution and measured using a Turner fluorometer. Pressure drop across the biocidal filters was monitored using a Magnehelic gauge.

E. TEST DESCRIPTION:

Various media provided by the Air Force Research Laboratory were tested, including biocide-treated and untreated media, in two thicknesses. Tests were carried out at three airflow rates under conditions of 50% relative humidity and room temperature. Glass-fiber filters were tested in parallel for comparison purposes.

F. RESULTS:

Significant capture efficiency greater than 97% was observed for both the iodine-treated and untreated media tested. In many cases, the efficiency was greater than 99%. There was no significant difference in capture efficiency between the iodine-treated and untreated filters. Efficiency decreased as particle size decreased. The pressure drop was initially around 3 in H_2O and increased as particles were collected on the filter, increasing blockage of air flow. The efficiency increased as filter thickness increased, as did pressure drop.

G. CONCLUSION:

The combined use of iodine disinfection and filtration is a technology that can potentially be used to capture and neutralize bioaerosols. Significant physical capture efficiency greater than 97% was observed for the biocide-treated media without a significant increase in pressure drop compared to a standard glass fiber filter tested under the same operating flow rates.

H. RECOMMENDATIONS:

Further analysis is needed to determine the sterilization capability of the biocide-treated media. Identification of the key disinfection mechanism is also of great importance. The media should also be tested for physical removal of microorganisms as well as for their ability to neutralize chemical agents.

AFRL/MLQ

TECHNICAL PUBLICATION / SECURITY AND POLICY REVIEW WORKSHEET

Public release clearance is not required for materials presented only in a closed meeting attended by authorized government personnel, to include government contractors, and materials presented are not placed in the public domain.

SECTION A. - COORDINATION: Completed from the top down.

DATE IN	TO	DATE OUT	APPROVED / DISAPPROVED	SIGNATURE
26 NOV 04	MLQL /PROJ MGR	26 NOV 04		
	MLQL /BRANCH CHIEF	2 Dec 04	Approved	
1 Dec 04	MLQO/FINANCE	1 Dec 04	APPROVED	
3 DEC 04	MLQO/OPSEC	6 DEC 04	Approved	
6 DEC 04	MLQO/PA	6 DEC 04	Approved	Wayne A Randall
7 Dec 04	MLQO/STINFO	7 Dec 04	Approved	
7 Dec 04	MLQ/CC	17 DEC 04	Approved	
7 Jan 05	MLQO/TIC	7 Jan 05	For DTIC Action	~~N/A~~

PA CASE NUMBER: *(PA use only)* 04 - 120

STINFO NUMBER: *(STINFO use only)*

SECTION B. - MATERIAL/PUBLICATION INFORMATION:

1. **IDENTIFICATION SUBMITTING ORGANIZATION:** (Name/Office Symbol/Ext)
   Joe Wander/MLQF/6240

2. **PRIOR CLEARANCES:** Have documents/materials been previously cleared for distribution / release? ☒ **YES** ☐ **NO** | If Yes; PA or TR Case #

3. **DOCUMENT TYPE:** (Submit only complete documents including all figures, charts, photographs and text.)
   ☐ Abstract ☐ Graphic ☐ Presentation/Brief ☐ Brochure ☐ Journal Article ☐ Speech ☐ Data
   ☐ News Release ☐ Success Story ☐ Display/Exhibit ☐ Technical Paper ☒ Technical Report ☐ Fact Sheet
   ☐ Other: _____

4. **MEDIA FORMAT:** ☐ CD-ROM ☒ Print/Paper ☐ Video ☐ Zip Disk ☐ Photo ☐ Poster ☐ Other: **.pdf**

5. **TITLE:** **Aerosol Capture by Iodinated Fiber Media**

6. **AUTHOR (S):** *(Last Name, First Name, MI, Rank/Grade - Lead Author First)*
   Ratnesar--Shumate, Shanna, Wanakule, Prinda, and Wu, C.Y.

7. **NAME OF JOURNAL OR DETAILS** *(Date and Place)* **OF ORAL PRESENTATION:** *(Include if Foreign)*
   AFRL tech report

8. PROJECT NO. (JON#)	9. CONTRACT NO.	10. PROGRAM ELEMENT:	11. WORK UNIT NO.
ARMT056W	F-08637-02-C-703002	63384D	~~DE~~

12. AUTHOR/CONTRACT MONITOR: *(Name/Office Symbol/Ext)*	13. CONTRACTOR:
Joe Wander/MLQF/3-6240	U of Florida, Dept of Environmental Eng. Science

14. **SECURITY CLASSIFICATION:** ☒ **Unclassified** ☐ **Other** ***(Specify)*** ☐ **Destruction Notice** ☐ **SBIR Report** ☐ **Phase I** ☐ **Phase II**

15. **LAST PUBLICATION FOR TEAM UNIT:** ☒ **YES** ☐ **NO** ☐ **INTERIM** ☒ **FINAL** | 16. **TR NUMBER:** **AFRL-ML-TY-TR-2004-4556**

17A. **DISTRIBUTION STATEMENT:** (AFI 61-204) *(Select distribution statement to be used and reason from below)*

☒ **A:** Approved for public release, distribution unlimited *(No reason required within section 17B.)*

☐ **B:** Distribution authorized to US Government agencies only *(reason) (date of determination)*. Other requests for this document shall be referred to *(controlling DoD office)*.

☐ **C:** Distribution authorized to US Government agencies and their contractors (reason) (date of determination). Other requests for this document shall be referred to *(controlling DoD office)*.

☐ **D:** Distribution authorized to Department of Defense and US DoD contractors only (reason) (date of determination). Other requests for this document shall be referred to controlling DoD office).

☐ **E:** Distribution authorized to DoD components only (reason) (date of determination). Other requests for this document shall be referred to controlling DoD office).

☐ **F:** Further dissemination only as directed by (controlling office) (date of determination) or DoD higher authority.

☐ **X:** Export Control: Distribution authorized to US Government agencies and private individuals or enterprises eligible to obtain export-controlled technical data in accordance with DoDD 5230.25 (date of determination). Controlling DoD office is (insert).

12-7-4

PREFACE

This report was prepared by the Aerosol and Particulate Research Laboratory, Department of Environmental Engineering Sciences, University of Florida, Gainesville, FL 32611-6450, under Contract Number F08637-02-C-7030 for the Air Force Research Laboratory (AFRL/MLQ), 139 Barnes Drive, Tyndall AFB, FL 32401-5323.

This is a final report being submitted to AFRL/MLQ. It describes work that was performed from November 02 to April 04. The Air Force Technical Program monitor was Dr. Joe Wander. We gratefully acknowledge the assistance of Triosyn® Corp, and Drs. Dale Lundgren and Samuel Farrah, at the University of Florida, without whom this study would not have been accomplished.

TABLE OF CONTENTS

TABLE OF CONTENTS (Continued)

LIST OF TABLES

LIST OF FIGURES

1.0: INTRODUCTION

1.1 Objective

The objective of this project was to evaluate the performance of an iodine/resin filter product developed by Triosyn®. In this phase of the study, the focus was on the physical capture efficiency for particles within the submicron-to-low-micron range. The ultimate goal is to utilize the iodine/resin filter technology for use as a protective gear for soldiers in the armed forces and for public and private buildings.

1.2 Background

1.2.1 Biological Warfare

As political differences intensify, the emerging threat of bioterrorism has escalated into a great concern for national security. The Center for Disease Control and Prevention defines bioterrorism as the *intentional or threatened use of viruses, bacteria, fungi, or toxins from living organisms to produce death or disease in humans, animals, or plants* (CDC, 2002). Among weapons of mass destruction, biological weapons are more destructive than chemical weapons and can be as devastating for human populations as nuclear weapons. For example, a few kilograms of anthrax (optimally delivered) could kill as many people as a Hiroshima-size nuclear bomb (Prescott et al., 2002). The use of biological warfare can be traced as far back as the 6th Century B.C., when Assyrians poisoned the wells of their enemies with rye ergot. During the 14th-Century siege of Kaffa, the Tartar army hurled plague-ridden corpses over the wall of the city, forcing defenders to surrender. During the 1940s there were several incidences of the Japanese releasing plague-causing bacteria that resulted in serious epidemics and death (FWG, 2004). In 1995 Aum Shinrikyo attempted on several occasions to release biological agents such as anthrax, botulinum toxin, Q fever, and Ebola in aerosolized form, their experiments killing at least 20 people and injuring thousands (CDC, 2004). In 2001 several anthrax-laced letters were sent through mail, killing five people in the United States. The anthrax spores sent out during these attacks were classified as being highly concentrated and processed to be disseminated and inhaled more easily (FWG, 2004).

In response to increased concern, in 1998 the United States Government launched a national effort to create a biological weapon defense program. Among the initiatives set forth by this program is the intent to invest in research and development in the science of biodefense (Prescott et al., 2002).

There are various methods commonly used to remove aerosols that are also applicable to removing biological aerosols from the air. Filtration, for example, has been effectively used to physically remove allergens such as pollen from the air. However, collected organisms may remain viable on filter surfaces. Given favorable humidity and temperature conditions for growth, the collected microorganisms may grow on collection media, and produce more undesirable bioaerosols. This phenomenon has been reported in many studies in heating, ventilation, and air conditioning (HVAC) systems (Nevalainen et al. 1993). For this reason it is important to deactivate microorganisms that are collected on filter media.

To be applicable for use by armed forces, a bioaerosol removal technology needs to meet additional requirements. It is necessary that it does not exert a high demand for consumable materials or require large amounts of energy to maintain. Bioaerosol removal technologies should be simple to install and operate, as well as being versatile, and able to operate in a wide range of conditions and to handle materials commonly present in battlefields. To be considered successful, the biodefense capability should not be compromised when other materials such as chemical weapons are present.

1.2.2 Bioaerosols

Bioaerosols are aerosols of biological origin. They can include living organisms such as bacteria and fungi, as well as non-living matter such as fungal spores, pollen, dust, allergens and, particularly, viruses. Bioaerosols typically range in size from about 0.02 μm for viruses to about 100 μm for pollen (Hinds, 1999). Many biological weapons utilize bioaerosols of an infectious agent because they are the most effective and efficient means to disperse the agents into the largest space in the shortest period of time.

Due to the unsuitability of air to act as a growth medium, any live bioaerosol that is airborne must have originated from a source such as humans, other animals, plants, food, soil, or water. Bioaerosols can occur as agglomerates, as clusters of organisms, as droplets, or attached to airborne debris such as dust (Prescott, 2002; Hinds, 1999).

Droplet nuclei are small particles about one to four micrometers (μm) that result from the evaporation of larger particles. Droplet nuclei can remain airborne for hours or days and travel long distances. If humans or animals are the source of bioaerosols, generally they are propelled from the respiratory tract into the air by coughing, sneezing, or vocalization. Large numbers of moisture droplets are aerosolized during a typical sneeze; each droplet can be about 10 μm in size and travel at up to 100 m/sec (Prescott, 2002). Airborne debris such as dust also acts as a route of transmission for aerosols. Bioaerosols can adhere to dust particles and become resuspended during disturbances (Prescott, 2002; Hinds, 1999)

1.2.3 Filtration

Due to the pathogenic nature of bioaerosols and the threat of biological weaponry, improving methods for effective capture and neutralization of airborne microorganisms is of great interest. One approach to controlling the concentration of bioaerosols and other particulate air contaminants is filtration (Maus et al., 2000). The type of air filter generally employed for filtration of bioaerosols is synthetic or glass fiber.

These filters typically collect aerosols, which consist of mineral dust particles or particles originating from various combustion sources, as well as bioaerosols. The mechanisms by which filtration captures particles are impaction, interception, and diffusion, of aerosols onto filter media. The capture efficiency of filters can depend on several factors including the size of the challenge aerosols, the filter fibers, the velocity of airflow through the filter, and the presence or absence of electric charge on the fibers or particles. Collection by interception occurs when a particle follows a gas streamline and comes in contact with the surface of a filter fiber. Inertial impaction occurs when a particle is captured due to its inertia and inability to adjust to changing streamlines near fiber surfaces. Impaction is the most important capture mechanism for larger particles since it is dependant on particle size and particle density. As velocity across a filter surface increases the capture by inertial impaction increases. Smaller particles are captured by diffusion to fiber surfaces caused by Brownian motion—random movement due to collision with gas molecules. As particle size decreases, capture by diffusion

increases. However, as flow velocity increases (*i.e.*, shorter retention time) capture efficiency due to diffusion decreases since particles have less time to travel towards fiber surfaces (Hinds, 1999).

Another factor is dependant on the physical properties of the microorganisms entering the filter. Bioaerosols often exists as clusters, and penetration by particles in clumps is less likely than by single-cell microbial particles (Wake et al. 1997). A significant fraction of airborne microorganisms are viable and retain viability after collection in air filters or other filtration devices. Concentrations of viable microorganisms in air filters can be as high as 10^3 colony-forming units (CFU) per gram and per square centimeter (Martikainen et al., 1990; Martiny et al., 1994). Due to this remaining viability, there is a large potential for microbial growth on filters under favorable conditions. The proper nutritional and moisture conditions may lead to microbial growth and then subsequent reentrainment from filter media. Other studies indicate that molds are able to grow on fibrous media if provided with 70–80% relative humidity and atmospheric dust (Maus et al., 2000). Spore-forming bacteria such as *Bacillus anthracis* are able to survive under extreme conditions and remain viable after filtration. However, under conditions of high relative humidity, RH> 80%, spore-forming bacteria may be negatively affected. Dehydration effects due to filtration may cause injury and death to collected microorganisms. Maus et al. (2000) found that rehydration of spores and the diffusion of fiber substances caused spores to become more susceptible to such environmental stress factors as airflow and air toxics, which then resulted in the loss of viability. It was found that bacterial and mold spores collected in air filter media are able to survive over prolonged periods of time and pose a potential for microbial growth, especially when humidity is high (RH>70%) and filters are not exposed to airflow. Abundant production and gradual release of spores into the clean air stream of the filters is likely to occur (Maus et al., 2000). Currently HEPA (High-Efficiency Particle Arresting) filters are used to control indoor air quality and can be worn as masks for the prevention of exposure to hazardous aerosols. However, there is a large pressure drop associated with the use of such filters that can lead to difficulty in breathing and high energy costs.

1.2.4 Iodine Disinfection

The halogens iodine and chlorine are antimicrobial agents of great importance (Prescott *et al.,* 2002). Halogen disinfection is a form of chemical sterilization in which oxidation of cell constituents and halogenation of cell proteins occurs (Prescott *et al.*, 2002). Iodine is a dark violet, non-metallic halogen element belonging to Group VIIA of the periodic table. Iodine is insoluble in water and when heated sublimes as a violet vapor. The melting point of iodine is 184.5°C and its molecular weight is 253.8 daltons. Iodine has been used as a disinfectant for potable water treatment, is used for on-site treatment of water, and is known for its chemical stability during storage (Brion and Silverstein, 1999). At high concentrations iodine has even been shown to kill some spores (Prescott, 2002). The I_2 disinfectant species is very stable in water over a *p*H range from 6 to 8. Iodine in the oxidation state of zero (I_2) is not highly soluble in water but may be introduced by heat vaporization, crystal dissolution, oxidation of iodide (I^{-1}), and release from iodine-containing resins or from the direct addition of high-strength iodine/alcohol solutions or triiodide (I^-_3) ions. The hypoiodous acid (HOI) form of iodine is thought to be the most effective for disinfection of viruses due to its +1 oxidation state. However elemental I_2 is thought to work better on cysts and bacteria. This is due to the time required to penetrate cell or cyst walls. Hypoiodous acid is unstable and quickly decomposes to form iodate (IO^-_3) and iodide (I^-). Iodine has the ability to bind to quaternary ammonium anion exchange resins as tri- or pent-iodide complexes (Brion and Sliverstein, 1999; Berg et al., 1964; Chang, 1958). These complexes are a demand-type disinfectant, releasing iodine in quantity only when needed, thus allowing for a longer product lifetime and minimizing casual exposure to iodine. While iodine is an excellent antimicrobial agent, overexposure to iodine can cause adverse health effects. The National Research Council recommends that exposure to iodine not exceed 150 micrograms per day (μg/day) (ASTDR, 2003). The major health effect of concern with excess iodine exposure by ingestion is thyroid disorders, primarily hypothyroidism (Backer and Hollowell, 2000). The use of activated carbon downstream of the iodinated resins is a possible method to remove excessive iodine from gas streams and eliminate negative health effects associated with exposure.

1.2.5 Iodine/Resin Filtration

The use of a filter in combination with an iodine resin product is used for potable water disinfection on spacecraft as well as for military personnel drinking water canteens. A new device termed the Microbial Check Valve (MCV) has recently been introduced for controlled release of I_2. The MCV is a canister that contains iodinated strong-base ion exchange resin beads. MCV resin binds polyiodide anions to quaternary ammonium fixed positive charges on a poly(styrene–divinylbenzene) copolymer anion exchange resin (Marchin *et al.*, 1997). Figure 1.1 shows the structure of a triiodide resin. The bound polyiodide anions release I_2 into water when they come in contact with suspended microorganisms, which results in devitalization of the microorganism.

Use of such an iodine/resin product in combination with filtration has been proposed for removal of bioaerosols. A biocidal resin developed by Triosyn Corp. is designed to minimize toxic effects of iodine to humans and the environment by controlling the delivery and dosage of free molecular iodine to microorganisms. The resin is produced by thermally fusing pure iodine crystals with a quaternary anion exchange polymer under high pressure. A stable ionic bond is formed between the iodine

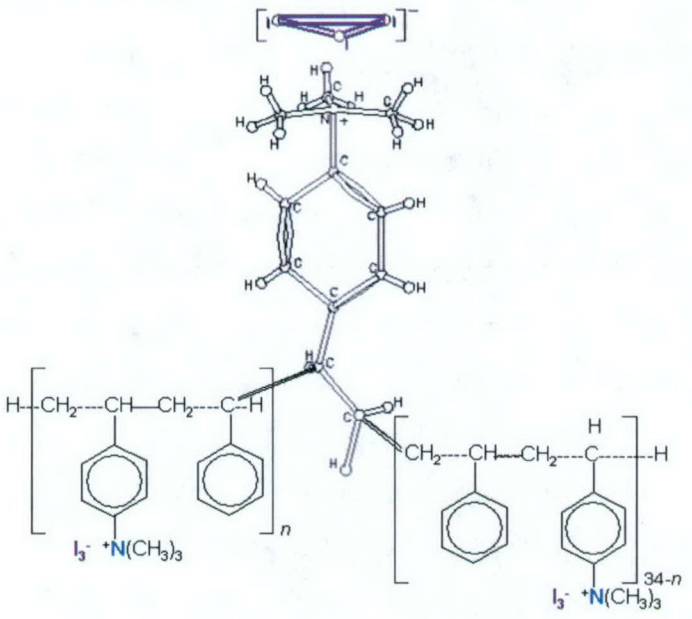

Figure 1.1 Chemical Structure of Triiodide Resin

and the resin polymer. This controls the release of free iodine for disinfection of microorganisms. Iodine molecules are then transferred from the resin to the strongly charged surface of microbial proteins, devitalizing by oxidation, hindering cellular functions.

However, there is limited research reported into the use of this product to disinfect air. According to a patent by Messier (2000), Triosyn® resin achieves high removal efficiency of microorganisms in air under various conditions. It was also reported that levels of iodine effluent in the air were less than the Threshold Limit Value of 1.0 mg/m^3 permitted during a period of 8 hrs, as set forth by the American Conference of Governmental Industrial Hygienists (Messier, 2000). According to a study performed by Triosyn®, airflow contaminated with the SARS corona virus was passed through a Triosyn® T-1000 Series Respirator, and no viable corona viruses were detected downstream (Triosyn, 2004).

Further evaluation of the Triosyn® iodine/resin product is needed to better understand the mechanisms by which this product operates. The physical removal of the microorganisms should be appraised to determine the efficiency of the use of resin-treated filters for the desiccation of microbes versus the use of iodine for disinfection on the filter substrate. Other key issues still to be explored are the effects of humidity and temperature on the disinfection performance of the iodinated resin. In a study performed by Messier, an increase in humidity decreased the number of viable microorganisms on glass rods (Messier, 1999). The report speculated that at higher humidity levels there will be an increase in the deactivation of aerosolized microorganisms on the iodine resin filter. This may be due to an increased release rate of iodine from the resin due to solubilization at high humidity. The report further speculated that increased temperature will increase disinfection efficiency due to an increase in iodine sublimation and reaction kinetics.

1.3 Scope

This report describes the performance and interpretation of experiments conducted at the University of Florida from November 2002 to April 2004 by Shanna Ratnesar–Shumate as part of the requirements for the Master of Science degree in environmental science and engineering.

2.0: APPROACH

There are two phases to this project. The first phase evaluated the physical capture efficiency of the iodinated-resin media, which is the focus of this report. The second phase looked at the viability, growth, and subsequent reentrainment of viable microorganisms from the iodinated-resin media under various operating conditions.

Several tasks were completed throughout the duration of this project:

- Design, construction, and testing of an experimental set-up for evaluation of physical capture efficiency of iodine treated and untreated filters.
- Calibration of a Turner Fluorometer 112 and determination of fluorescent backgrounds due to cuvette irregularities, and filter interference.
- Testing of several types of filters, iodine-treated, untreated, and filters of different thickness.
- Testing of capture efficiency of filters at different flow rates.

The following chapters elaborate the procedures and methods used to complete this research project.

3.0: EXPERIMENTAL

3.1: Particle Generation

3.1.1: Selection of Model Aerosol

When conducting research employing aerosols, it is imperative to find a model aerosol that can be used for experimental purposes. It is desired that such model aerosols be spherical in nature and have uniform density, thus allowing for a convenient method of mass concentration determination (Stöber and Flachsbart, 1973).

Spherical latex particles in liquid suspension are a widely used material for this sort of analysis. Polystyrene latex (PSL) particles offer several advantages when used for calibration procedures involving microscopic counting and sizing measurements. However, the use of latex particles for size-related mass concentration proves to be difficult for many reasons. As latex particles are generated from liquid suspensions using atomizers, at high concentrations more than one latex particle may be suspended in a water droplet; upon evaporation, agglomerates or clusters of more than one particle may exist. Therefore, to prevent large clumps from forming during calibration work involving latex particles, very low concentrations of particles in suspension must be used, thus increasing sampling times needed to accumulate a significant amount of particles for gravimetric analysis (Stöber and Flachsbart, 1973).

For the purposes of aerosol research, a solution to this is to disperse a suitable substance to generate particles directly rather than dispersing a suspension of particles. This method allows for particle formation from every droplet produced, decreasing sampling time. However particles obtained using this method are polydisperse, requiring the use of particle sizing analysis. A disadvantage to using solution-generated particles is that ideal spherical particles are no longer generated. Small crystals or irregular crystalline aggregates may form, as shown by Walkerhorst and Dautrebande (1964) for inorganic salts such as sodium chloride (Stöber and Flachsbart, 1973).

Uranine, the sodium salt of fluorescein, has been used in a number of studies. This chemical emits a strong fluorescence that can be measured using fluorometers and permits sensitivity measurement at concentrations of 10^{-9} g/cm^3 in conventional fluorometers. However, uranine is hygroscopic, and therefore its use can lead to a

misinterpretation of data since analysis is based on rehydration of samples in an ammonium hydroxide solution in water.

Ammonium fluorescein, the ammonium salt of fluorescein, is used for similar fluorometric analyses and is not hygroscopic. Stöber and Flachsbart (1973) showed that ammonium fluorescein particles emerging from a nebulizer dry up and form spherical particles of uniform density within a short time after mixing with clean air of low humidity. Although solubility in water is low, this study found that dissolving fluorescein in aqueous ammonia allows a sensitive mass determination by fluorometric measurements under ultraviolet (UV) irradiation (Stöber and Flachsbart, 1973).

To evaluate the physical capture efficiency of the iodinated-resin media, ammonium fluorescein particles were employed due to the lower detection limit of fluorescence compared to gravimetric measurements. Figure 3.1 displays a schematic diagram of the entire experimental set-up for Phase I of this project and Figure 3.2 shows the photographs taken of the system. A 6.75-g/L fluorescein solution in 0.1 *N* NH_4OH was aerosolized by a six-jet modified Collison Nebulizer (Model # CN25, BGI Inc.). This concentration was chosen to allow for the production of larger particles and enhanced detection. A dilution dryer in combination with dry air flow was used to evaporate the droplets into solid fluorescein particles (May, 1972)

3.2: Flow Control

In a study performed by Triosyn, a flow rate of 85 Lpm was used across a filter surface area of 100 cm^2. The flow rates for these experiments were scaled down to achieve the same face velocity through the 17.35-cm^2 filter area used in this study as Triosyn used. Three flow rates were evaluated: 15 Lpm—which corresponds in face velocity to the 85 Lpm used in Triosyn's tests—and 13 and 21 Lpm, which were used for comparison. Flow was controlled using calibrated rotameters placed at various points within the system. Air was passed through the nebulizer at a flowrate of 10 Lpm and dilution air was introduced into the dilution drier chamber at twice this amount to ensure adequate moisture conditions. An excess airflow point was used to control the flow going through the target filter and maintain the flow rates at the designated levels of 13, 15, and 21 Lpm, respectively.

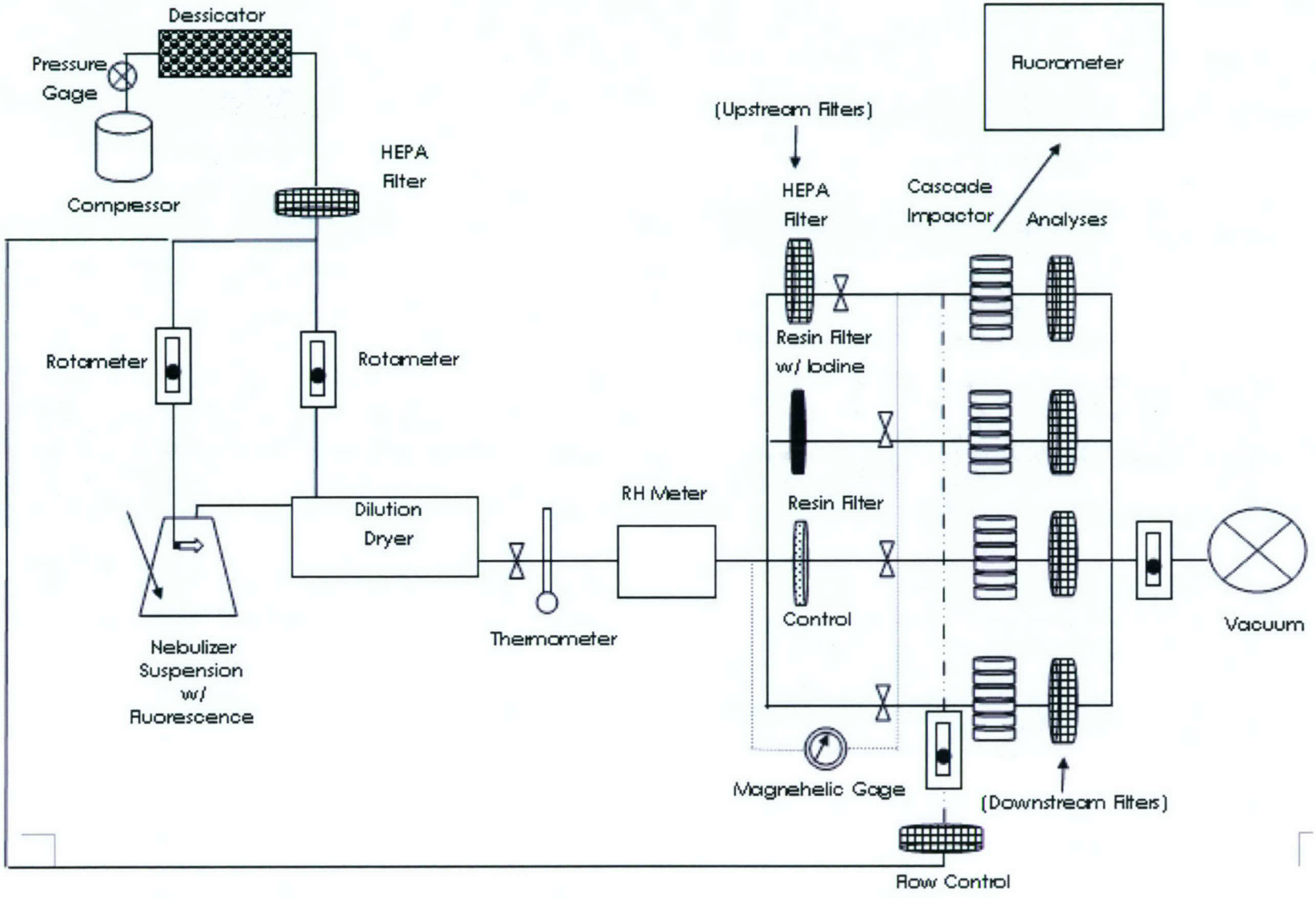

Figure 3.1 Schematic of Experimental Set-up

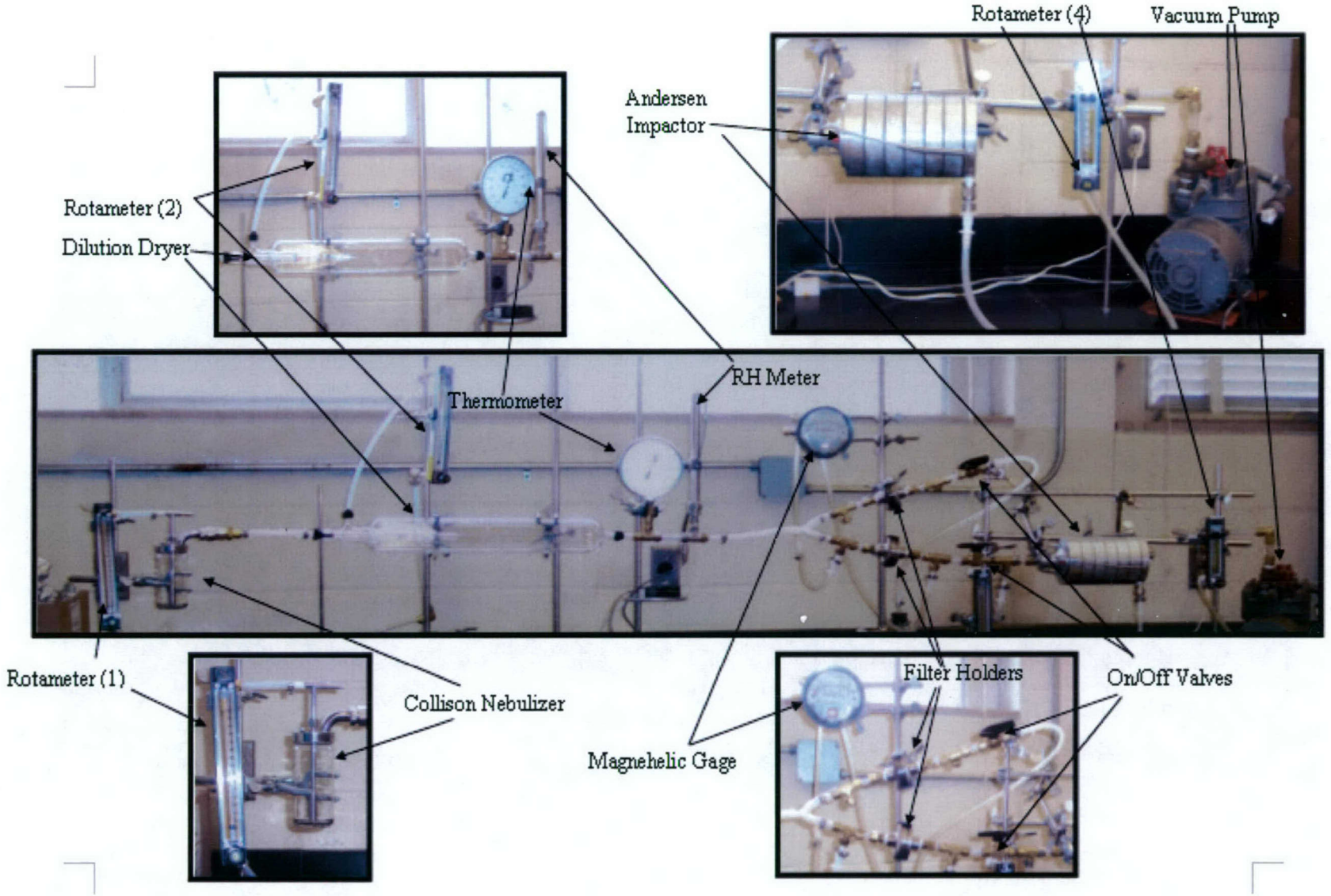

Figure 3.2 Photographs of the Experimental Set-up

3.3 Particle Capture and Size Classification

3.3.1 Inertial Impaction

Cascade inertial impactors are instruments used to measure particle size distribution by mass. They work by passing aerosols following a gas stream through a nozzle; the output stream (jet) is directed towards a flat plate. As seen in Figure 3.3, the impaction plate redirects the flow to form an abrupt 90° bend in the gas streamline. Due to particle inertia, large particles unable to follow the gas streamlines will impact on the plate's surface. A sticky surface on the plate can be used to ensure that particle bouncing does not occur. Smaller particles that are able to follow the streamlines remain airborne and flow out of the impactor. Particles larger than a certain aerodynamic size are deposited from the air stream, and those smaller than that size pass through the impactor, thus sorting themselves by size (Hinds, 1999).

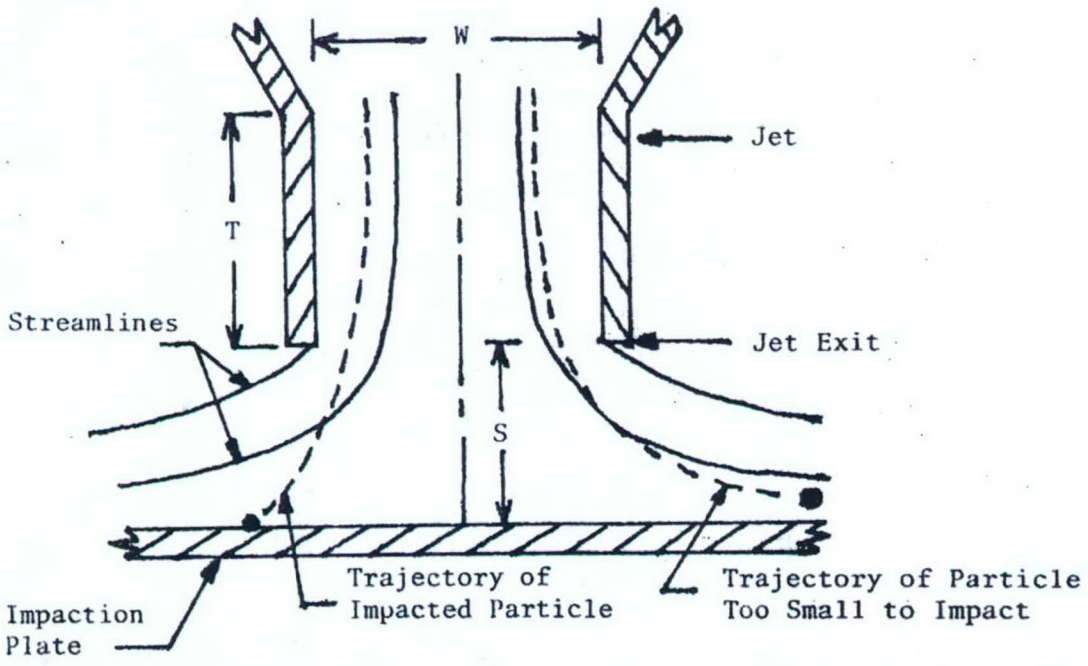

Figure 3.3 Cross-sectional view of an impactor (Source: US EPA)

As shown in Figure 3.4 a cascade impactor comprises several impactors in series, arranged in order of decreasing cut-off size. In an ideal impactor, the cut-off size or d_{50} is the size than which all particles of greater aerodynamic size are collected and all particle of smaller size pass through. The cut-off size is reduced at each stage by

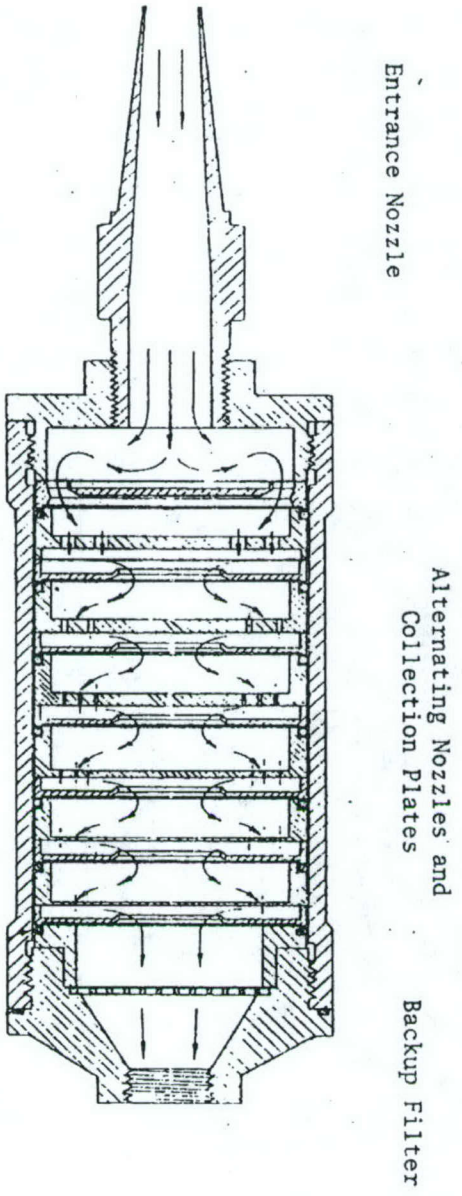

Figure 3.4 Cross-Sectional View of a Cascade Impactor Schematic Diagram. (Source: US EPA)

decreasing the nozzle diameter, which increases the flow velocity through the jet. The same flow rate is maintained through the cascade impactor. The last stage in a cascade impactor is generally followed by a filter that captures all particles smaller than the cut-off size of the last stage.

The size range of particles collected on each stage is based on the jet velocity of the stage and the cutoff size of the previous stage. Particles not collected on a stage follow the air stream around the impactor plate to the next stage. Collection of particles by a surface is a function of inertial impaction parameters:

$$Stk = \frac{C\rho_d U D_p^{\,2}}{9\mu D_c}$$

Where Stk_{50} is the Stokes number for 50% collection efficiency for impactors (0.24 for circular jets), U is the flow velocity, ρ_d is the particle density, D_p is the particle diameter in μm, μ is the gas viscosity, D_c is the diameter of the round jet, and C is the Cunningham slip correction factor. The Cunningham slip correction factor is equal to

$$C = 1 + 0.16 \bullet 10^{\,4} / D_p$$

for normal temperatures and pressures. This factor corrects for the condition that a particle's diameter approaches the mean free path length of gas molecules, thus the particles "slip" between gas molecules more easily and tend to cross between flow streamlines (Thermo Electron Corp, 2003). Cut size can be calculated based on the following relationship (Hinds, 1999), where Q is the jet flow rate:

$$d_{50}\sqrt{C} = \sqrt{\frac{18\mu\pi D_c^{\,3}(Stk_{50})}{4\rho_p Q}}$$

3.3.2 Andersen Impactor

Penetrating aerosols leaving the iodinated-resin media were captured and classified by particle size on a six-stage Andersen impactor, shown in Figure 3.5(a). The Andersen Viable Particle Sampler is constructed with six aluminum stages that are held together by three spring clamps and sealed with *O*-ring gaskets. Each impactor stage contains jet orifices that are precision drilled. As air is drawn though the sampler, multiple jets of air on each stage direct any airborne particles toward the surface of the impactor plates.

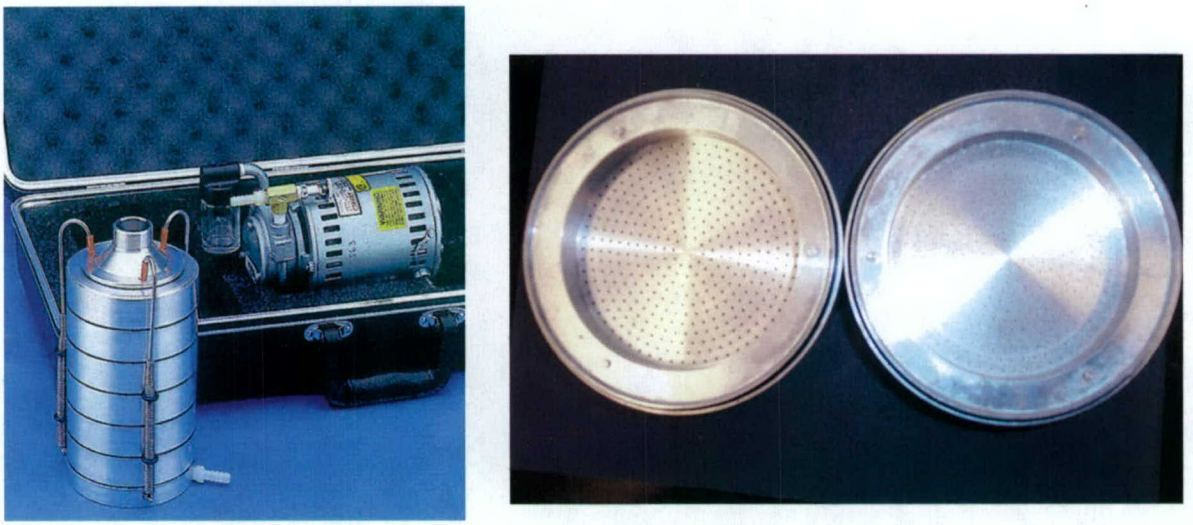

(a) (b)

Figure 3.5 (a) Photographs of Andersen six-stage impactor (b) Example of stage jet orifices and varying jet sizes, at left- stage 1, at right -stage 5

The size of the jet orifices is constant on each stage and varies from stage to stage, going from larger to smaller in each succeeding stage. Figure 3.5(b) shows stages 1 and 5. Each stage contains 400 jet orifices with diameters ranging from 1.81 mm on the first stage to 0.25 mm on the sixth stage (see Table 4.1). Plates for each stage of the impactor were coated with 10% by mass Apiezon-L® grease in toluene and baked for 2 hrs at 70°C to create a sticky surface for prevention of particle bouncing. The Andersen impactor was run at 28.3 Lpm and dilution air was also introduced into the system prior to entering the impactor to maintain 28.3 Lpm. The corresponding size range for each stage is listed in Table 3.1. Figure 3.6(a) shows samples collected on stage six

Table 3.1: Stage Number, Size Range and Jet Diameter for Thermo Andersen Impactor at 28.3 Lpm

Stage no.	1	2	3	4	5	6	DF
Size Range (μm)	20–7.1	7.1–4.7	4.7–3.3	3.3–2.1	2.1–1.1	1.1–0.65	<0.65
Jet Diameter (mm)	1.1958	0.9205	0.7143	0.5382	0.3469	0.2569	----

[a] DF=downstream filter

(Thermo Electron Corp, 2003). A 47-mm Millipore glass fiber filter (Lot # H3NN53241) was used downstream of the final impactor stage to collect any remaining particles. Although other cascade impactors may provide finer resolution in the submicron range, this impactor was chosen because of its capability for bioaerosol sampling, which other impactors do not possess.

3.4 Pressure Drop

Pressure drop is due to the resistance to airflow across a filter. Pressure drop represents the total drag force of all the fibers in a filter. Pressure drop is directly proportional to flow rate; this is due to the flow inside most filters' being laminar. When considering filtration it is ideal to have a medium that provides the highest collection efficiency with the smallest pressure drop. In fibrous filters pressure drop increases as particles accumulate on the medium. Pressure drop across a filter is important for several reasons (Hinds, 1999). High pressure drop in ventilation systems leads to higher energy requirements and can be uneconomical. Filters used for protective gear that have a high pressure drop can result in difficult breathing, which can impair performance and limit endurance. According to the manufacturer of the glass filters used in comparison to the Triosyn filters (see Appendix D), the expected pressure drop across the Millipore AP15 series at 15 Lpm is 22 in H_2O, (Millipore, 2004). Pressure drag is a measure of the filter aerodynamic resistance to air flow and can be calculated by dividing pressure drop across a filter by filtration velocity (Noll, 1999).

A Magnehelic gage reading 0–10 in H_2O was employed to evaluate the pressure drop across the iodinated-resin media. A Magnehelic differential pressure gage indicates the difference in pressure between two input connections. A reading was taken every minute for each run.

3.5 Sample Rehydration

After collection, the individual stages containing fluorescein particles were rehydrated in aqueous 0.1 *N* NH_4OH solution and then treated with methylene chloride to dissolve the grease coating on each plate. The individual stages containing fluorescent particles were immersed in 20 mL of methylene chloride to dissolve the grease coating on each plate and sonicated for 10 minutes. After sonication, 20 mL of 0.1 *N* NH_4OH was

added to each sample and poured into a test tube. Due to the immiscibility of methylene chloride and ammonium hydroxide, a fluorescein–ammonium hydroxide solution separated to the top of each sample while the methylene chloride, containing the grease, sank to the bottom. The top layer of each sample was then pipetted into quartz cuvettes for analysis. Concentrations of fluorescein solution from each stage were measured using a fluorometer (G.K. Turner Associates). Figure 3.6(b) displays fluorescein solutions in the fluorometer. This analysis was used to determine the particle size distribution based on mass concentration for uncaptured particles after filtration with the filters. Both iodine-treated media and untreated media were evaluated to look for possible differences in morphology of the media based on the ion-exchange treatment and for consequent differences in capture efficiency. To determine dependence of capture efficiency on thickness, two medium thicknesses were also evaluated. Each experiment was run for 15 minutes. This amount of time was shown to be sufficient to deliver a measurable amount of fluorescent particles for evaluation, while not causing a mound effect due to accumulation of particles under each impactor jet, which would alter the calibration of the Andersen impactor. The experimental conditions are listed in Table 3.2.

(a) **(b)**

Figure 3.6 (a) Impactor Plate after Run; Yellow Dots Are Clusters of Fluorescein Particles Collected; (b) Fluorescent Solution in Cuvette in Fluorometer During Analysis

Table 3.2: Operating Parameters for All Experiments							
Experiment Number	Flow Rate (Lpm)	Upstream Filter	Downstream Filter	Concentration of Fluorescein in 0.1 *N* NH_4OH (g/L)	Run Time (min)	Temp (°C)	Barometric Pressure (in. Hg)
12–14	21	Glass Fiber (Millipore Lot # H3NN53241)	Glass Fiber (Millipore Lot # H3NN53241)	6.75	15	25	30.20
15–17	21	None	Glass Fiber (Millipore Lot # H3NN53241)	6.75	15	25	30.20
18–20	21	Triosyn Iodine Coated (PTM 002 Lot # 120903-01)	Glass Fiber (Millipore Lot # H3NN53241)	6.75	15	23	30.25
21–23	21	Triosyn Uncoated (PTM 002 Lot #120903-02)	Glass Fiber (Millipore Lot # H3NN53241)	6.75	15	23	30.19
24–26	15	Glass Fiber (Millipore Lot # H3NN53241	Glass Fiber (Millipore Lot # H3NN53241)	6.75	15	24	30.23
27–29	15	None	Glass Fiber (Millipore Lot # H3NN53241)	6.75	15	24	30.23
30–32	15	Triosyn Iodine Coated (PTM 002 Lot # 120903-01)	Glass Fiber (Millipore Lot # H3NN53241)	6.75	15	23	29.20
33–35	15	Triosyn Uncoated (PTM 002 Lot #120903-02)	Glass Fiber (Millipore Lot # H3NN53241)	6.75	15	22	29.20
36–38	13	Glass Fiber (Millipore Lot # H3NN53241	Glass Fiber (Millipore Lot # H3NN53241)	6.75	15	23	30.20
39–41	13	None	Glass Fiber (Millipore Lot # H3NN53241)	6.75	15	23	30.10
42–44	13	Triosyn Iodine Coated (PTM 002 Lot # 120903-01)	Glass Fiber (Millipore Lot # H3NN53241)	6.75	15	23	---
45–47	13	Triosyn Unoated (PTM 002 Lot #120903-02)	Glass Fiber (Millipore Lot # H3NN53241)	6.75	15	23	---
48–50	15	Triosyn Iodine Coated (LMFEXP Lot # 120903-01)	Glass Fiber(Millipore Lot # H3NN53241)	6.75	15	23	---

4.0 RESULTS

4.1 Morphological Analysis

As shown in Figure 4.1, scanning electron microscopic (SEM) pictures were taken of untreated Triosyn filters prior to beginning experimentation. A dense woven structure of long fibers was observed by visual analysis. The filter fibers are of different thicknesses, which may enhance capture of different-size particles.

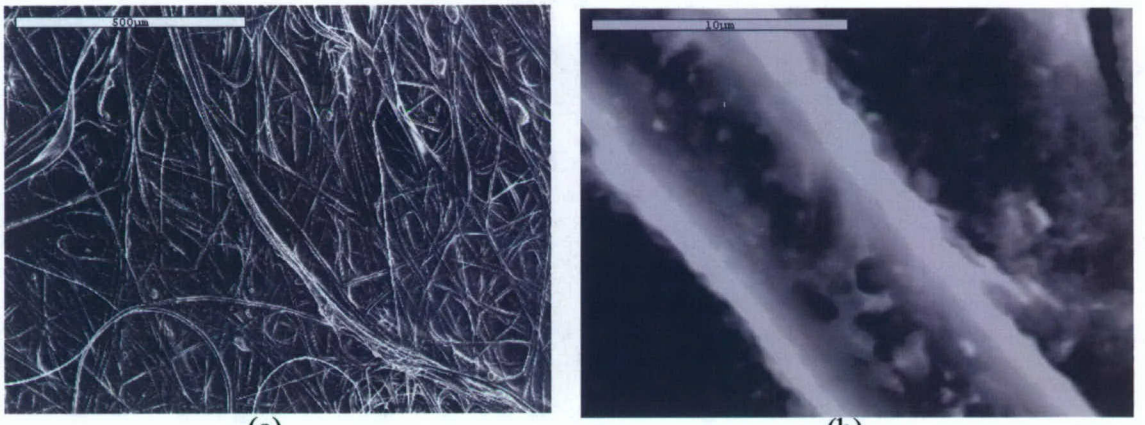

(a) (b)

Figure 4.1 SEM Images of Triosyn (Non-treated) Filters (a) 5100X (b) 54000 X

Figure 4.2 shows photographs of the same Triosyn filters, taken with a digital optical microscope. Note small solid objects visible in these photographs. The resin fibers appear semi-transparent, and vary significantly in thickness.

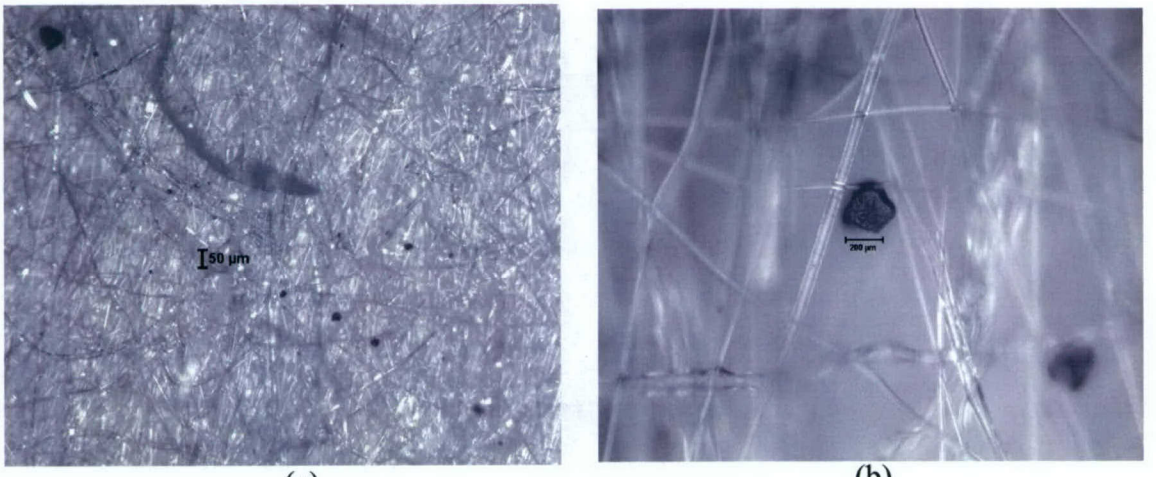

(a) (b)

Figure 4.2(a)(b) Digital Optical Microscopic Pictures Taken of Triosyn (Untreated) Filters (a) 55X (b) 520X

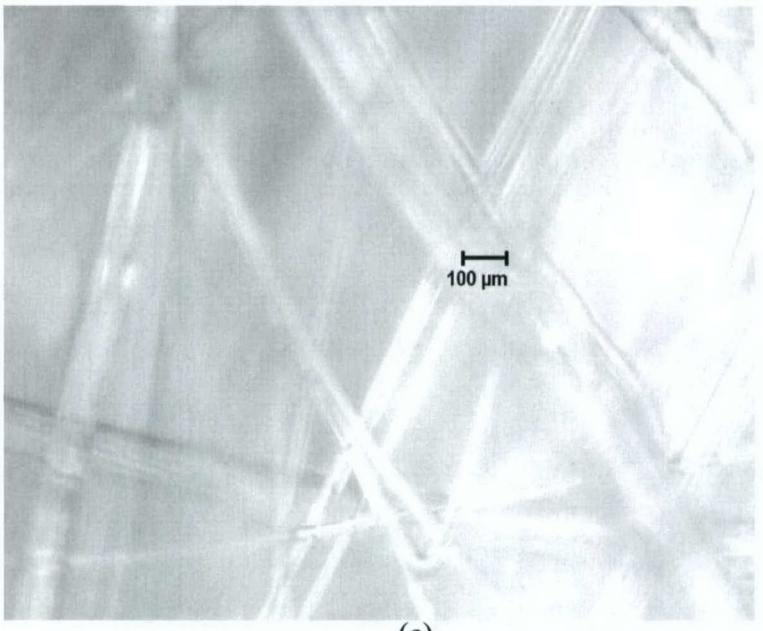

(c)

Figure 4.2(c) Digital Optical Microscopic Pictures Taken of Triosyn (Untreated) Filter at 550X Magnification

4.2 Fluorometer Calibration

A Sequoia–Turner 112 Digital Filter Fluorometer was used to measure the mass concentration of particles that landed on each stage of the impactor. The instrument is used to measure fluorescence of materials caused by absorbed radiation. A calibration of concentration vs. fluorometer reading was performed using samples of known fluorescein concentration in 0.1 *N* NH_4OH. The calibrations were performed for four different gain settings: 1X, 3X, 10X, 30X, where the larger the gain setting the lower the concentration detectable by the fluorometer. Fluorometer readings less than 30 and higher than 100 are considered to be less reliable; therefore, to obtain the most accurate readings possible, the range settings were selected to match the concentration of the solution being analyzed. Figure 4.3 shows the linear relationship between concentration and fluorometer reading at different range settings that were used to analyze the samples for this study. Detailed calibration results are presented in Appendix A.

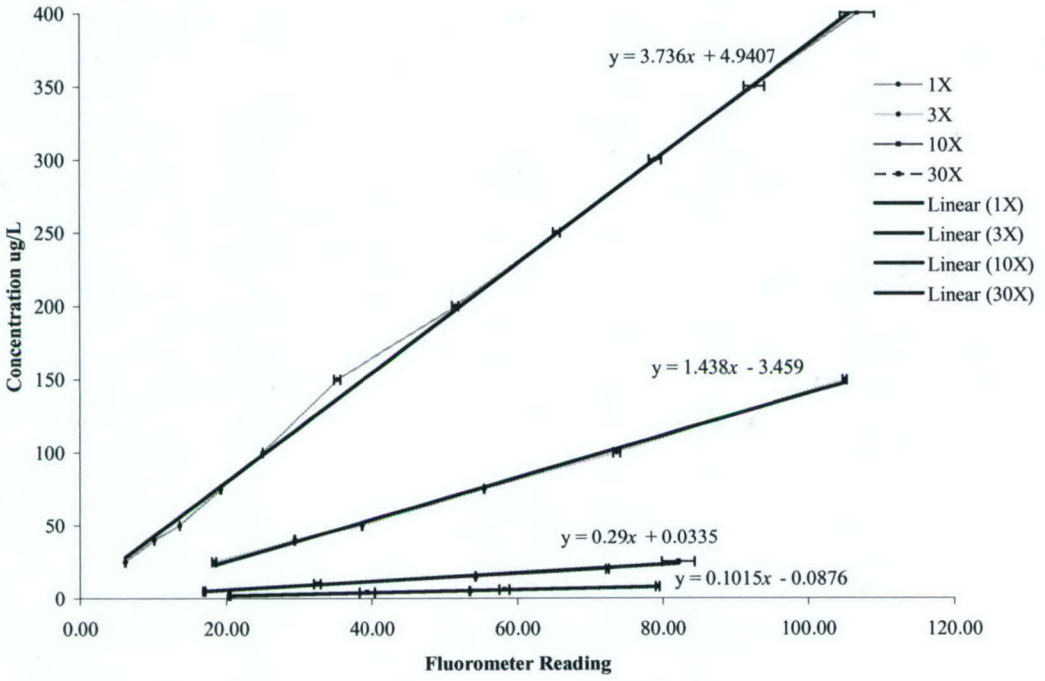

Figure 4.3 Linear Calibration Curve of Turner 112 Fluorometer

4.3 Particle Size Distribution

The average size distribution of particles produced within the system reaching the point of filtration was determined during control runs at 13, 15 and 21 Lpm using no medium upstream of the impactor. The results are shown in Figure 4.4. The majority of the fluorescent particles were collected on the downstream filter stage (<0.65 μm) and the fifth and sixth stages (1.1–0.65 and 2.1–1.1 μm) for each flow rate. The shape of the distribution has a similar pattern for different flow rates, while the total mass increased as the flow rate increased, as expected. Due to the low concentration of detectable particles on stages 1–4 the data for these stages were not used (see Appendix B for data).

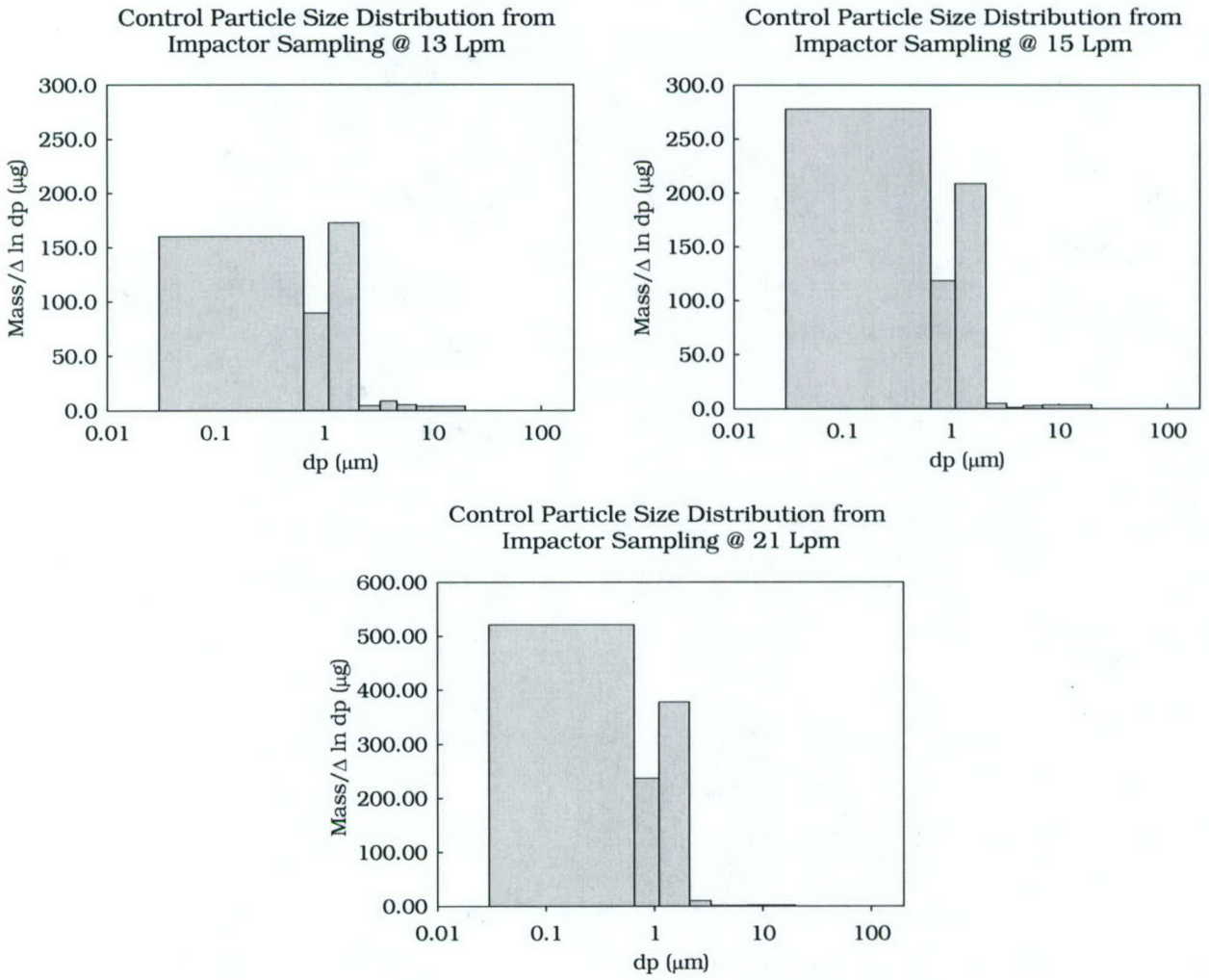

Figure 4.4: Average Particle Size Distribution Based on Mass of Particles Collected on Impactor with No Filter Upstream

4.3.1 Filter Fluorescence and Cuvette Background

Many factors may skew results of fluorometric analysis, *e.g.*, fluorescence given off by reagents, filter substances reacting with chemicals, or flaws within different cuvettes used in analysis. For this reason several background tests for the various filter media were conducted. The results shown in Table 4.1 clearly prove there was no interference by the filter media on fluorescence analysis from the glass fiber and blank

Table 4.1: Background Fluorescence Levels for Filters	
Filter Type	**Corresponding Background Fluorescence as μg of Fluorescein**
Glass Fiber	0.06
Blank Triosyn PTM 002	0.03
Iodine Treated	$B = 0.1423x\text{-}113.22$ (where x is total mass detected, and B is skewed mass)

Triosyn filters. However a negative interference was observed for the iodine-treated Triosyn filters. The interference may be attributed to chemical reaction occurring between the iodine and fluorescein in the rehydrated filter solution. The data for iodine-treated filter media initially showed less capture efficiency than the blank treated media. This was due to a negative fluorescence appearing when samples containing hydrated iodine-treated filters were analyzed, which led to interpretations of lower mass concentrations on the upstream filter than were actually collected. Since mass fraction capture depends on the mass of fluorescein captured on the upstream filter, compared to the downstream impactor stages, capture efficiency appeared to be less than expected. After performing a calibration to determine the relative negative interference of iodine with fluorescence predicted for concentration of fluorescein in a sample, a concentration-based interference curve was established and used to adjust the values listed in Table 4.2.

Table 4.2 Capture Efficiency % Per Stage				
Stage#	**5**	**6**	**DF**	**Total**
Size Range (μm)	**2.1–1.1**	**1.1–0.65**	**0.65–0.03**	**-**
Iodine @ 13 Lpm	99.86± 0.0111	99.96± .0292	99.22± 0.167	**99.34± 0.118**
Blank @ 13 Lpm	99.91± 0.00447	99.79± 0.0263	99.12± 0.184	**99.62± 0.830**
Iodine @ 15 Lpm	99.81± 0.00509	99.21± 0.0464	96.84± 0.0634	**97.32± 0.381**
Blank @ 15 Lpm	99.89± 0.0328	99.87± 0.0234	99.38± 0.101	**99.43± 0.0826**
Iodine @ 21 Lpm	99.99± 0.000308	99.51± 0.0199	98.85± 0.149	**99.01± 0.0877**
Blank @ 21 Lpm	99.93± 0.0320	99.53± 0.0308	98.95± 0.263	**99.07± 0.191**
Thick Iodine @ 15 Lpm	99.94± 0.00276	99.97± 0.00191	99.50± 0.126	**99.56± 0.0904**

Variations in the optical properties of each cuvette were also investigated to determine the overall effect on data reproducibility. The results are displayed in Appendix C. A maximum standard deviation of 0.8% was observed at 500 μg/L (the maximum concentration that was readable by the Turner fluorometer) based on fluorometer readings of different cuvettes oriented at different directions at differing concentrations. Therefore it can be concluded, for the purposes of this project, that cuvette differences did not affect analysis by fluorometry.

4.4 Capture Efficiency of Iodine/Resin Filters

The size distribution results for the experiments performed using Triosyn filters upstream are presented in Figure 4.5. The filters tested were Triosyn iodine-treated PTM002 Lot # 120903-1, Triosyn untreated PTM002 Lot # 120903-2, at 13, 15 and 21 Lpm, and Triosyn iodine-treated thick LMFEXP Lot# 120903-01 at 15 Lpm. Table 4.2 summarizes the capture efficiency for particles at each stage of the impactor. Each value is the average of three tests. It should be noted that data for stages 1–4 should be ignored because of the low concentration level relative to the background level. A significant removal, consistently greater than 97% was observed for both the iodine-treated and blank Triosyn filters tested for stages 5 and 6 and for the downstream filter (DF). Figure 4.6 is a picture of the filters taken after sampling and rehydration. It was observed that some amount of fluorescence was not captured by the upstream Triosyn filter. When similar experiments were performed using glass fiber filters upstream, no detectable fluorescence was observed on the downstream filters, indicating that the glass fiber filters have higher removal efficiency than the Triosyn filters. Figure 4.7 is photographs taken of the re-hydrated solutions in test tubes prior to pipetting into cuvettes. It can be noted from these photographs that when the glass fiber filters were located upstream, no visible fluorescence was observed. Efficiency greater that 99.8% was observed for 1.1–2.1-μm particles for all flow rates tested. The efficiency decreased to <99% for particles smaller than 0.65 μm and to 96.84% for the iodine-treated filters tested at 15 Lpm. For the larger particles (1.1–2.1 μm), impaction is the important mechanism. Hence, increasing the flow velocity (21 Lpm vs. 13 Lpm) resulted in higher efficiency. On the

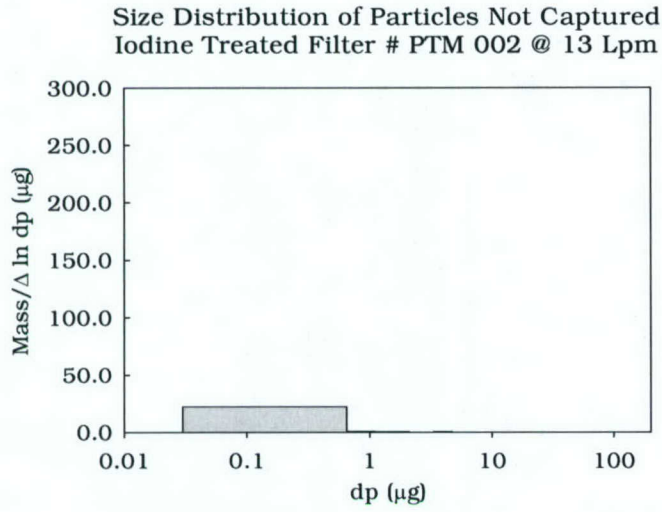

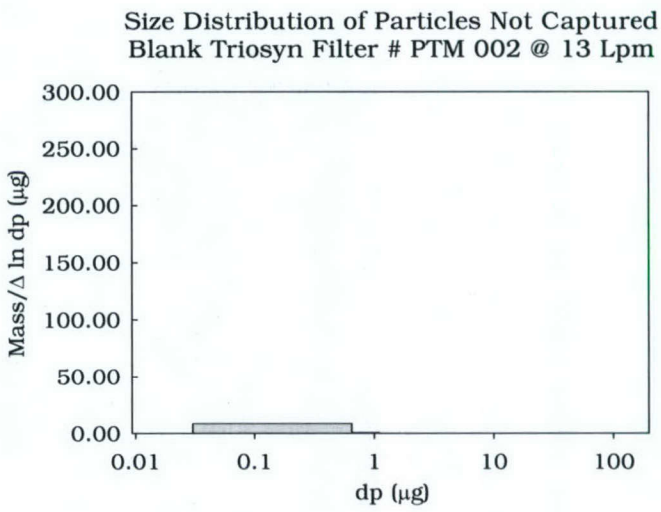

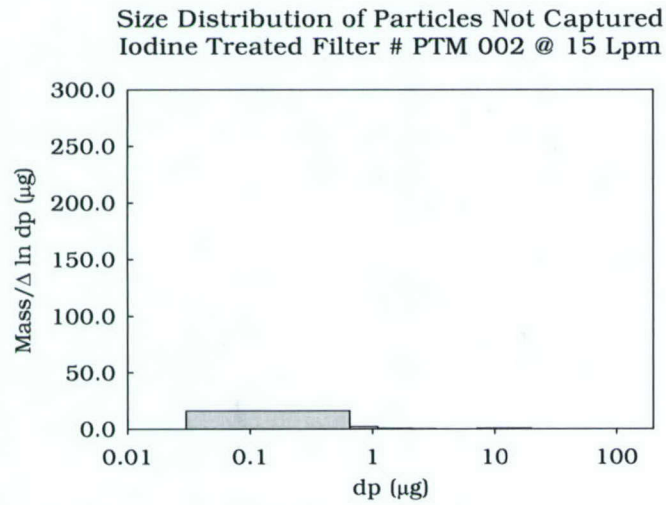

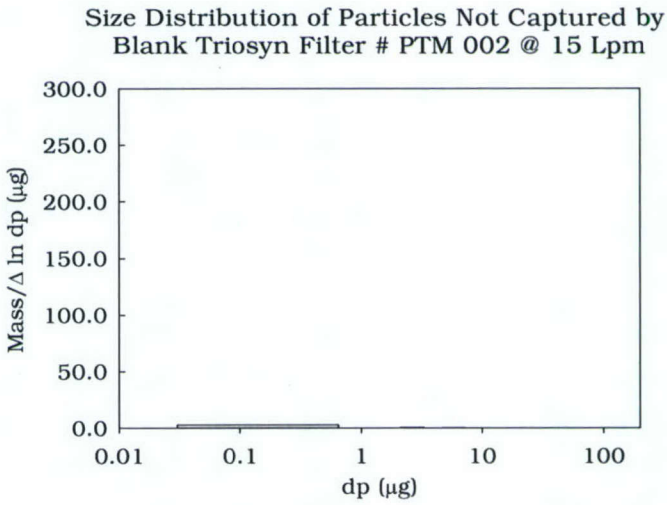

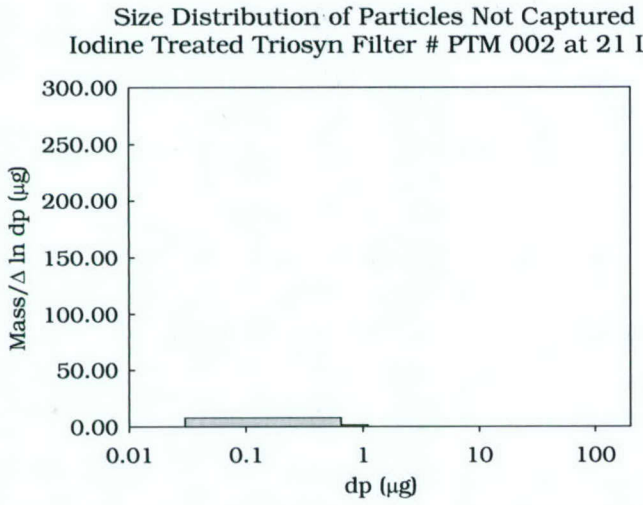

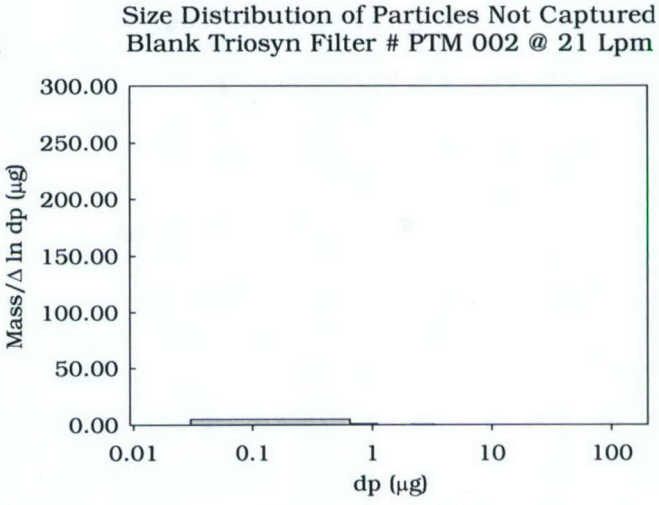

Figure 4.5 Average Particle Size Distribution Based on Mass of Particles Collected on Impactor with Triosyn Filters Located Upstream

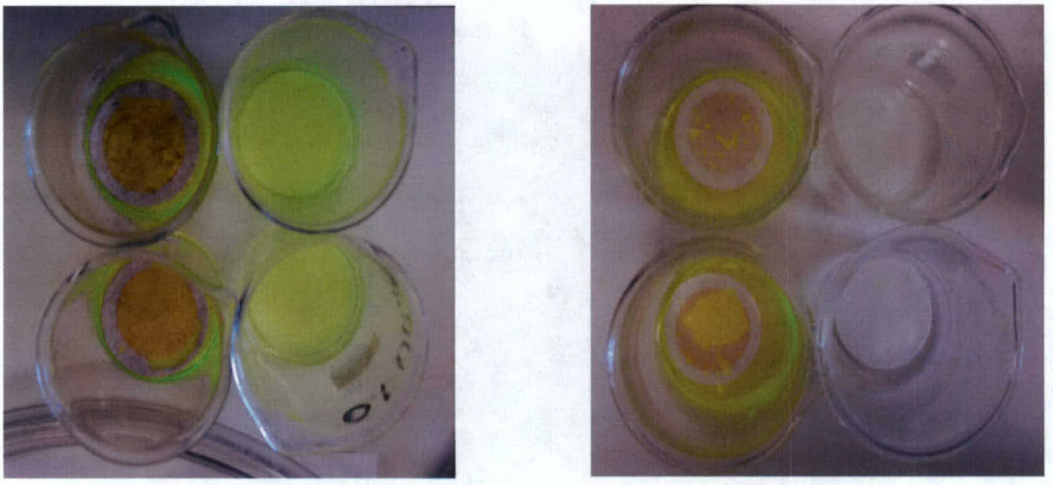

(a) (b)

Figure 4.6 Filters after hydration (a) right are iodine treated Triosyn filters that were located upstream of the impactor, left are glass fiber filters that were located downstream of the impactors (b) right are glass fiber filters that were located upstream of the impactor, left are glass fiber filters that were located downstream of the impactors.

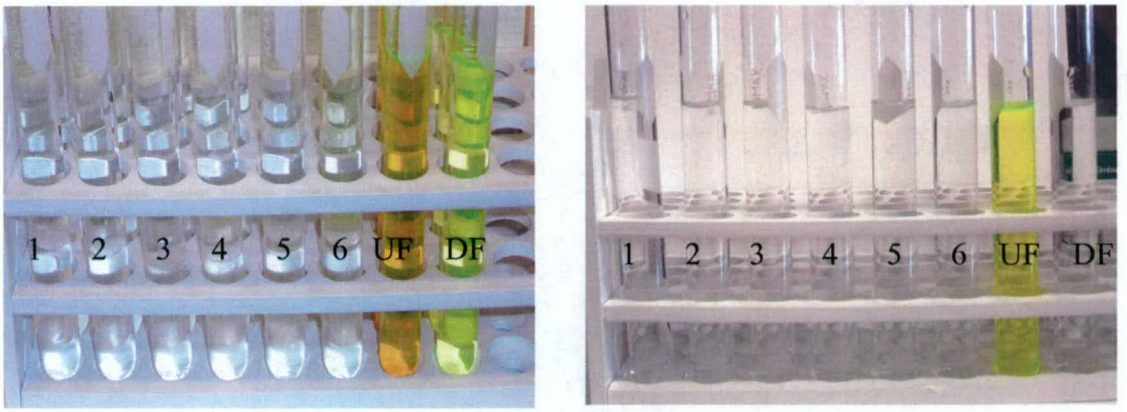

(a) (b)

Figure 4.7 Rehydration Solutions Before Measurement in the Fluorometer, from Left to Right Starting at Stage 1 Through 6 and Then the Upstream and Downstream Filters (a) Triosyn Filters Upstream (b) Glass Fiber Filters Upstream

other hand, capture by diffusion is the dominant mechanism for smaller particles (<0.65 μm). A higher flow rate resulted in a shorter retention time for diffusion and consequently lower collection efficiency. The highest capture efficiency was generally observed in the 1.1–2.1-μm range and efficiency decreased as the particle size decreased. Both treated and untreated filters appeared to perform similarly based on the data, which

showed no significant difference. The thick filters did appear to perform better than the regular iodine-coated filters at 15 Lpm, which was expected due to the increased possibility for impaction and longer retention time leading to greater diffusion of particles to fiber surfaces.

4.5 Pressure Drop

Pressure drop across the three types of media being tested (iodine treated, untreated, and thick iodine treated) was recorded. The system was tested with and without the use of the aerosolized particles to determine how particle accumulation on the filter affected pressure drop. A pressure drop of 0.2 in H_2O was observed when no medium was inserted into the filter holder, which we attributed to the wire mesh backing that was placed behind the media samples for support. When the nebulizer was on, and particles flowed through the testing filters and were captured, pressure drop increased from initial values of 1.8 in H_2O at 15 Lpm and 2.3 in H_2O for 21 Lpm to beyond the range of measurement (see Figure 4.8). Notably, pressure drop reached beyond the measurable range more quickly at higher flow rates, which is most likely due to the increased rate of accumulation of particles on the filter surface. The initial pressure drop of the Triosyn filters was significantly less than the associated pressure drop of the glass fiber filters tested (22 in H_2O). Comparison was also made based on filter drag (= pressure drop/flow velocity). The Triosyn filters had a filter drag of 0.0055 in H_2O/(in/min), which was much lower than that of the glass fiber filter (0.066 in H_2O/(in/min)) (details in Appendix D).

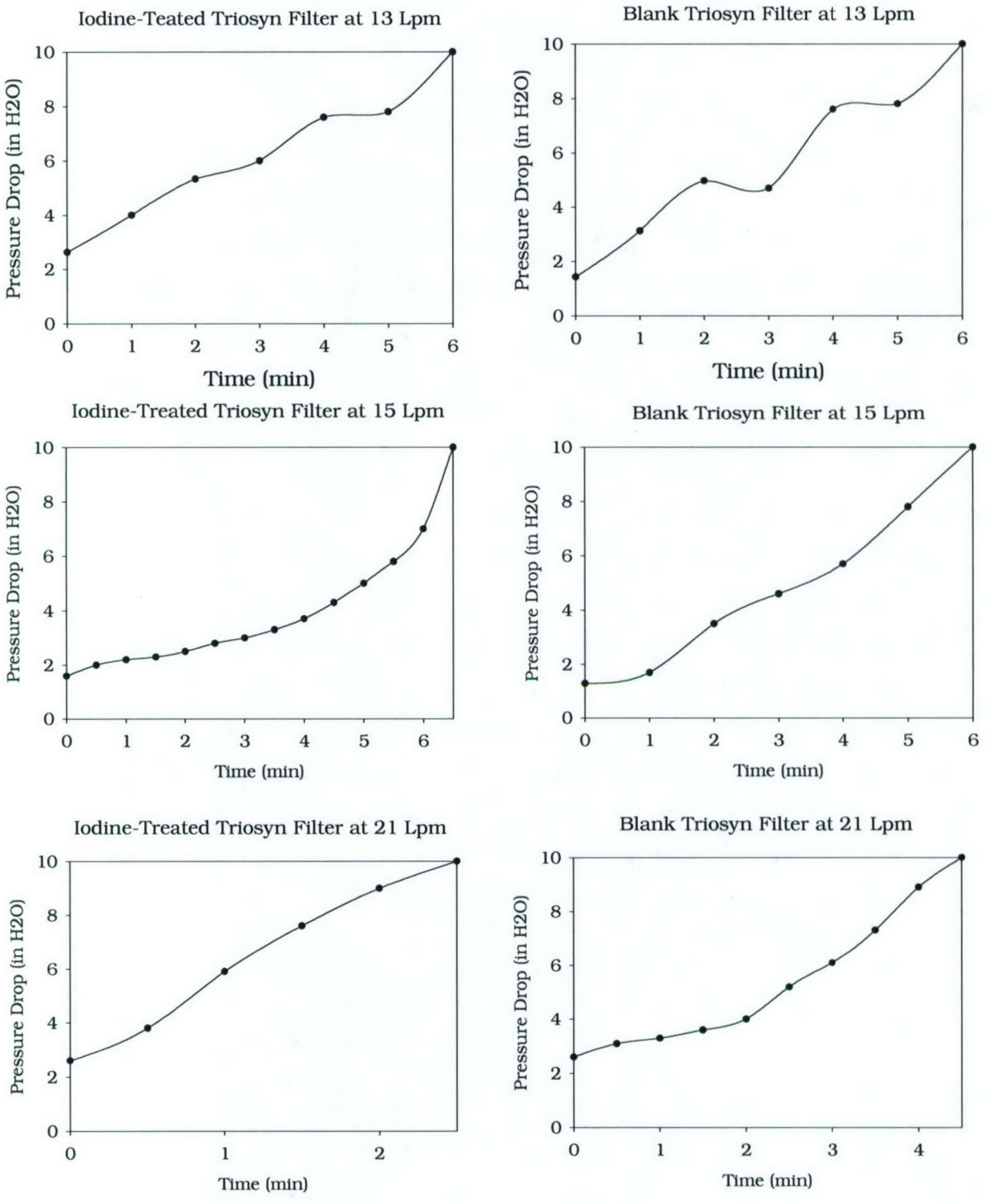

Figure 4.8 Pressure Drop as a Function of Time for the Iodine-Treated and Blank Filters for Three Flow Rates

5.0 SUMMARY, CONCLUSIONS AND RECOMMENDATIONS

5.1 Summary

The objective of this phase of study was to evaluate the physical capture efficiency of a novel biocidal filter material developed by Triosyn®. A filtration testing system was designed and constructed that can generate and characterize aerosols of a wide size range. This experiment was performed using ammonium fluorescein particles as the test aerosols that were passed though the filters being tested. All particles not captured by filtration were classified by a cascade impactor for analysis. Significant capture (>97%) by the filters was observed for a wide particle size range; in most cases the efficiency was greater than 99%. However, a fraction of fluorescein particles were still detected visually and fluorometrically downstream of the biocidal and blank media. For larger particles (1.1–2.1 μm) the efficiency was the highest and it increased slightly as flow velocity increased since impaction is the main collection mechanisms for this size range. For the smaller particles (<0.65 μm collected in downstream filter), the efficiency was the lowest and it decreased as flow velocity increased. Diffusion is the main collection mechanism for the smaller particles and its efficiency depends on retention time. The thicker filter has a better efficiency due to increased possibility for impaction and larger retention time for diffusion. The difference however was not great because the baseline filter already had a higher efficiency. Pressure drop across the Triosyn media was shown to be less than across the glass fiber medium, but increased as the particle layer built up. Pressure drop was shown to increase the fastest at 21 Lpm, which is expected due to the increased rate of accumulation of particles on the filter. No relationship between iodine-treated, or untreated filters and pressure drop was observed.

5.2 Conclusions

Several conclusions were drawn based on this study: 1) the biocidal media did not show a significant difference in the capture efficiency compared to the blank medium. 2) Overall, capture efficiency increased as particle size increased, with the highest efficiency being observed in the 1.1–2.1-μm range. 3) Pressure drop across the biocidal

filters was initially less than across the glass fiber filters tested for comparison. 4) The iodinated-resin media are not as efficient at physical removal of aerosols as glass fiber media, but efficiency greater than 97% was achieved with a much lower pressure drop.

5.3 Recommendations

It is recommended that further studies be performed on these filters to evaluate the actual disinfection capability of the biocidal filters. Viable bioaerosols should be used to determine if they are deactivated as they pass through the iodine/resin filters. Several different microorganisms that have the potential to be used for biological weaponry should be tested, including viruses, bacteria, and fungi. The effects of humidity and temperature should also be determined to establish the optimal operating conditions or limitations for this new technology. Another important aspect that should be looked into is the interaction between potential chemicals used for chemical warfare and how they might hinder the effectiveness of the biocide filters, or possible chemical reactions that may occur that may be harmful to personnel wearing such protective gear. Furthermore an overall better understanding of the disinfection mechanisms between the iodine resin and the microorganisms should be investigated, to enable optimal use of this technology.

REFERENCES

ATSDR (Agency for Toxic Substances and Disease Registry). *Iodine: CAS # 7553-56-2.* Division of Toxicology TOX FAQs. September 2001.

Backer, H., Hollowell, J. "Use of Iodine for Water Disinfection: Iodine Toxicity and Maximum Recommended Dose." *Environmental Health Perspectives*. 108: 679–684.

Berg, G., Chang, S. L., Harris, E.K. (1964). "Devitalization of Microorganisms by Iodine." *Virology*. 22:469–481.

Brion, M.G., Silverstein, J. (1999). " Iodine Disinfection of a Model Bacteriophage MS2, Demonstrating Apparent Rebound." *Water Research.* 23: 169–179.

Chang S.L. (1958). "The Use of Iodine for the Disinfection of Water." *Journal of the American Pharmaceutical Association*. 48:417–423.

Environmental Protection Agency (US EPA). (1980). *Use and Limitation of In-Stack Impactors*. Environmental Sciences Research Laboratory. EPA-600/2-80-048. pp. 13–14.

Hinds, C. W. (1999). *Aerosol Technology*. John Wiley & Sons, New York, pp. 394–400.

Martikainen, P.J., Asikainen, A., Nevalainen, A., Jantunen, M., Pasenen, P., Kalliokoski, P. (1990). "Microbial Growth on Ventilation Filter Materials." *Proceedings of the Fifth International Conference on Indoor Air Quality and Climate.* 3:203–206.

Martiny, H., Mortiz, M., Ruden, H. (1994). "Deposit of Bacteria and Fungi in Different Materials in Air Conditioning Systems." *Proceedings of the International Symposium on Cont. Control.* pp. 203–206.

Maus, R., Goppelsöroder, A., Umhauer, H. (2000). "Survival of Bacterial and Mold Spores in Air and Filter Media." *Atmospheric Environment.*35:105–113

May, K.R. (1972). "The Collison Nebulizer: Description, Performance and Application." *Journal of Aerosol Science.* 4:235–243.

Messier, P.J. (1999). *Disinfection of Air Using an Iodine/Resin Disinfectant*. US Patent No. 5980827.

Messier, P.J. (2000). *Iodine/Resin Disinfection and Procedure for the Preparation Thereof.* US Patent No. 6045820.

Millipore (2004) *Glass Fiber Filters. Technical Information*. www.millipore.com. .

Munro, L. (1999) *Essentials for Microbiology Laboratory*. Contemporary Publishing Company. Raleigh, N.C., p.71

Nevalainen, A., Willeke, K., Liebhaber, F., Pastuszka, J., Burge, H. and Henningson, E., "Bioaerosol Sampling" in *Aerosol Measurement*, Eds. Willeke, K. and Baron, P., Van Nostrand Reinhold, New York, 1993.

Noll, Kenneth. (1999) *Fundamentals of Air Quality Systems. "Pressure Drop"* American Academy of Environmental Engineers. pp. 173–174

Prescott, M. L., Harley, P.J.,Klein, A.D. (2002). *Microbiology*. McGraw–Hill, New York. pp. 147–148, 856, 863.

Stöber, W., Flachsbart, H. (1973). "An Evaluation of Nebulized Ammonium Fluorescein as a Laboratory Aerosol." *Atmospheric Environment*. 7:737–748.

Wang, Z., Reponen, T., Grinshun, A.S., Rafal, L.G. (2001). "Effect of Sampling Time and Air Humidity on the Bioefficiency of Filter Samples for Bioaerosol Collection." *Journal of Aerosol Science*. 32:661–674.

Wake, D., Bowry, C., Crook, B., Brown, C. (1997). "Performance of Respirator Filters and Surgical Mask Against Bacterial Aerosols." *Journal of Aerosol Science*. 28:1311–1329.

West, R.C. (1983–1984) *CRC Handbook of Chemistry and Physics. 64th Edition*. CRC Press Inc. p. D-196

Web References

Forth Worth Government. *History of Biological Terrorism*. www.fortworthgov.org/health/threats/bio_history1.asp 1 September 2004.

Center for Disease Control. *Historical Trends Related to Bioterrorism: An Empirical Analysis*. www.cdc.gov/ncidod/EID/vol5no4/tucker.htm. 1 September 2004.

Center for Disease Control. *Collaboration Between Public Health and Law Enforcement: New Paradigms and Partnerships for Bioterrorism Planning for Response*. www.cdc.org. 13 February 2003.

Cleaning.Com. *An Innovation for Global Clean Water.* http://www.cleaning.com/news/nasagwater.php4. 25 April 2003.

Oregon State.University *Disinfection of Water.* http://oregonstate.edu/atwaterj/h20.dis 25 April 2003.

Triosyn. *What is Triosyn Resin?* www.triosyn.com.technology.php. 30 September 2004.

Appendix A

Calibration Data for Sequoia–Turner 112 Digital Filter Fluorometer

Fluorometer Setting (1X)

Analysis One:					
ug/L	**Readings 1X**	**Readings 1X**	**Readings 1X**	**Readings 1X**	**Average**
400	105.4	105.00	105.2	105.1	105.18
350	91.6	91.70	91.5	91.8	91.65
300	78.3	78.50	78.4	78.4	78.40
250	65.8	65.80	65.8	65.8	65.80
200	51.2	51.40	51.1	51.1	51.20
150	34.9	34.90	34.9	34.9	34.90
100	25	25.00	25	25	25.00
75	19.2	19.20	19.2	19.2	19.20
50	13.6	13.60	13.6	13.6	13.60
40	10.1	10.10	10.1	10.1	10.10
25	6.2	6.20	6.2	6.2	6.20

Analysis Two:					
ug/L	**Readings 1X**	**Readings 1X**	**Readings 1X**	**Readings 1X**	**Average**
400	108.7	108.40	108.4	108.4	108.48
350	93.6	93.80	93.8	93.3	93.63
300	79.6	79.60	79.6	79.6	79.60
250	65.1	65.10	65	65.1	65.08
200	51.9	51.90	51.7	51.7	51.80
150	35.5	35.50	35.5	35.5	35.50
100	25	25.00	25	25	25.00
75	19.3	19.30	19.3	19.3	19.30
50	13.6	13.60	13.6	13.6	13.60
40	10.1	10.10	10.1	10.1	10.10
25	6.1	6.20	6.1	6.2	6.15

Concentration (ug/L)	**Average Reading 1X**	**Standard Deviation**
400	106.83	2.33
350	92.64	1.40
300	79.00	0.85
250	65.44	0.51
200	51.50	0.42
150	35.20	0.42
100	25.00	0.00
75	19.25	0.07
50	13.60	0.00
40	10.10	0.00
25	6.18	0.04

Fluorometer Setting (3X)

Analysis One:					
ug/L	Readings 3X	Readings 3X	Readings 3X	Readings 3X	Average
150	105.3	105.20	105.2	105.2	105.23
100	73.3	73.30	73.3	73.3	73.30
75	55.4	55.50	55.4	55.5	55.45
50	38.7	38.70	38.7	38.7	38.70
40	29.4	29.40	29.4	29.4	29.40
25	18.6	18.60	18.6	18.3	18.53

Analysis Two:					
ug/L	Readings 3X	Readings 3X	Readings 3X	Readings 3X	Average
150	104.9	104.80	104.8	104.8	104.83
100	74.2	74.30	73.3	74.2	74.00
75	55.4	55.40	55.4	55.4	55.40
50	38.6	38.60	38.6	38.6	38.60
40	29.3	29.30	29.3	29.3	29.30
25	18.1	18.10	18.1	18.1	18.10

Concentration (ug/L)	Average Reading 3X	Stand Deviation
150	105.03	0.28
100	73.65	0.49
75	55.43	0.04
50	38.65	0.07
40	29.35	0.07
25	18.31	0.30

Fluorometer Setting (10X)

Analysis One:					
ug/L	Readings 10X	Readings 10X	Readings 10X	Readings 10X	Average
25	83.9	83.80	83.5	83.5	83.68
20	72.3	72.20	72.2	72.2	72.23
15	54.1	54.30	54.3	54.3	54.25
10	33.1	32.60	32.7	32.7	32.78
5	16.9	16.90	16.8	16.8	16.85

Analysis Two:					
ug/L	Readings 10X	Readings 10X	Readings 10X	Readings 10X	Average 10X
25	80.5	80.50	80.5	80.5	80.50
20	72.5	72.50	72.5	72.5	72.50
15	54.2	54.20	54.2	54.2	54.20
10	32.1	32.10	32.1	32.1	32.10
5	17	17.00	17	17.3	17.08

Concentration (ug/L)	Average Reading 10X	Standard Deviation
25	82.09	2.25
20	72.36	0.19
15	54.23	0.04
10	32.44	0.48
5	16.96	0.16

Fluorometer Setting (30 X)

Analysis One:							
ug/L	**Readings 30X**	**Readings 30X**	**Readings 30X**	**Readings 30X**	**Readings 30X**	**Readings 30X**	**Average**
8	82.6	80.50	79.2	78.3	78	75.8	79.07
6	60.2	60.20	59.1	58.3	57.6	56.6	58.67
5	53.5	53.50	53.5	53.4	53.4	53.4	53.45
4	40.7	39.80	38.7	38.4	37.2	36.6	38.57
2	20.6	20.20	20.2	20.2	20.2	20.2	20.27

Analysis Two:							
ug/L	**Readings 30X**	**Readings 30X**	**Readings 30X**	**Readings 30X**	**Readings 30X**	**Readings 30X**	**Average**
8	80.5	80.50	78.8	78.8	78.8	79.3	79.45
6	57.9	57.90	57.8	57.9	57.4	57.4	57.72
5	53.4	53.40	53.4	53.4	53.4	53.4	53.40
4	39.8	39.80	40.1	40.1	40.1	40.1	40.10
2	20.5	20.50	20.5	20.5	20.5	20.5	20.50

Concentration (ug/L)	**Average Reading (30X)**	**Standard Deviation**
8	79.26	0.27
6	58.19	0.67
5	53.43	0.04
4	39.33	1.08
2	20.38	0.16

Appendix B

Experimental Data

Experimental Data Run @ 13 Lpm

Control Filter w/ Upstream Glass Fiber			
Stage	Mass #36 (ug)	Mass # 37 (ug)	Mass # 38 (ug)
1	0.157	0.157	0.116
2	0.014	0.147	0.183
3	0.195	0.104	0.108
4	0.627	0.207	0.043
5	0.126	0.457	0.112
6	0.057	2.093	0.020
Ufilter	3802.435	1371.696	1791.592
Dfilter	2.145	1.805	0.556
Total	3805.755	1376.665	1792.731

Control Filter w/ No Upstream Glass Fiber			
Stage	Mass #39 (ug)	Mass # 40 (ug)	Mass # 41 (ug)
1	1.101	4.981	0.736
2	1.518	3.147	6.069
3	2.265	4.821	5.157
4	0.848	0.963	3.267
5	75.633	75.633	63.113
6	79.554	90.866	108.410
Dfilter	466.421	n/a	520.966
Total	627.341	180.412	707.718

Iodine Coated Triosyn Filter			
Stage	Mass #42 (ug)	Mass # 43 (ug)	Mass # 44 (ug)
1	0.139	0.199	0.257
2	0.056	0.193	0.256
3	0.167	1.277	0.704
4	0.167	0.421	0.157
5	0.258	0.972	0.405
6	0.235	1.920	0.820
Ufilter	3914.497	3359.705	4523.346
Dfilter	28.186	22.209	16.622
Total[1]	29.208	27.190	19.222

[1]Sum of Stages 1-6 and Dfilter

BlankTriosyn Filter			
Stage	Mass #45 (ug)	Mass # 46 (ug)	Mass # 47 (ug)
1	0.175	0.182	0.312
2	0.192	0.184	0.804
3	0.152	0.118	0.198
4	0.185	0.502	0.250
5	0.183	0.484	0.239
6	0.851	1.786	0.532
Ufilter	2706.542	3192.222	3199.694
Dfilter	10.266	3.516	12.979
Total[1]	12.003	6.772	15.314

[1]Sum of Stages 1-6 and Dfilter

Experimental Data for Runs @ 15 Lpm

Control Filter w/ Upstream Glass Fiber			
Stage	Mass #24 (ug)	Mass # 25 (ug)	Mass # 26 (ug)
1	0.167	0.265	0.166
2	0.113	0.313	0.250
3	0.071	0.151	0.163
4	0.126	0.169	0.199
5	0.091	0.193	0.202
6	0.329	0.187	0.354
Ufilter	1455.100	1098.476	1337.184
Dfilter	0.151	0.316	0.146
Total	1456.148	1100.069	1338.664

Control Filter w/ No Upstream Glass Fiber			
Stage	Mass #27 (ug)	Mass # 28 (ug)	Mass # 29 (ug)
1	1.771	0.952	2.723
2	1.849	1.153	2.795
3	0.263	1.288	0.303
4	1.331	2.296	1.774
5	87.415	90.003	81.088
6	152.988	122.790	92.879
Dfilter	705.525	711.502	1150.244
Total	951.142	929.984	1331.807

Iodine Coated Triosyn Filter			
Stage	Mass #30 (ug)	Mass # 31 (ug)	Mass # 32 (ug)
1	0.524	0.175	0.353
2	0.301	0.121	0.283
3	0.233	0.101	0.234
4	0.182	0.149	0.151
5	0.469	0.229	0.262
6	2.428	2.473	1.239
Ufilter	2127.146	1729.630	1841.328
Dfilter	70.926	40.963	37.526
Total[1]	75.063	44.212	40.048

[1]Sum of Stages 1-6 and Dfilter

BlankTriosyn Filter			
Stage	Mass #33 (ug)	Mass # 34 (ug)	Mass # 35 (ug)
1	0.208	0.157	0.224
2	0.161	0.190	0.505
3	0.103	0.110	0.207
4	0.456	0.158	0.386
5	0.184	0.178	0.164
6	0.043	0.044	1.055
Ufilter	1417.712	2348.577	2188.480
Dfilter	8.281	8.684	11.560
Total	9.436	9.520	14.101

[1]Sum of Stages 1-6 and Dfilter

Experimental Data for Runs @ 21 Lpm

Control Filter w/ Upstream Glass Fiber			
Stage	Mass #12 (ug)	Mass # 13 (ug)	Mass # 14 (ug)
1	0.340	0.044	0.133
2	0.209	0.035	0.051
3	0.033	0.057	0.049
4	0.037	0.036	0.084
5	0.066	0.045	0.039
6	0.061	0.045	0.053
Ufilter	920.164	1618.073	2547.546
Dfilter	0.148	0.310	---
Total	921.056	1618.645	2547.955

Iodine Coated Triosyn Filter			
Stage	Mass #18 (ug)	Mass # 19 (ug)	Mass # 20 (ug)
1	0.034	0.006	0.016
2	0.049	0.007	0.003
3	0.331	0.100	0.015
4	0.032	0.000	0.004
5	0.019	0.000	0.011
6	2.158	1.875	1.495
Ufilter	3040.446	2527.947	2593.652
Dfilter	27.065	27.439	20.677
Total[1]	29.688	29.428	22.221

[1]Sum of Stages 1-6 and Dfilter

Control Filter w/ No Upstream Glass Fiber			
Stage	Mass #15 (ug)	Mass # 16 (ug)	Mass # 17 (ug)
1	2.021	0.860	1.357
2	0.603	0.960	1.484
3	1.564	0.523	0.423
4	5.481	2.834	3.085
5	175.229	212.521	80.800
6	271.958	271.958	194.306
Dfilter	1164.624	1629.577	2021.672
Total	1621.480	2119.233	2303.127

BlankTriosyn Filter (NEW)			
Stage	Mass #21 (ug)	Mass # 22 (ug)	Mass # 23 (ug)
1	0.063	0.052	0.050
2	0.063	0.072	0.046
3	0.058	0.062	0.163
4	0.147	0.459	0.089
5	0.115	0.133	0.149
6	1.403	1.562	0.611
Ufilter	2211.488	1661.213	1777.212
Dfilter	18.491	19.057	9.834
Total[1]	20.339	21.397	10.943

[1]Sum of Stages 1-6 and Dfilter

Experimental Data for Thick Filter Runs @ 15 Lpm

Thick Filters			
Stage	Mass #49 (ug)	Mass # 50 (ug)	Mass # 51 (ug)
1	0.986	0.477	0.244
2	0.524	0.346	0.150
3	0.179	0.248	0.174
4	0.149	0.315	0.184
5	0.144	0.089	0.261
6	0.069	0.180	0.180
Ufilter	3149.168	4349.796	3251.591
Dfilter	17.628	12.394	11.560
Total[1]	19.679	14.050	23.703

[1]Sum of Stages 1-6 and Dfilter

Appendix C

Cuvette Background Calibration

➢ **Note: T_{12},T_3, T_6,andT_9 Represent the 4 sides of each circular cuvette.**

Concentration (ug/L)	**500.0**														
Power Setting	**1x**														
	Cuvette # 1					**Cuvette # 2**					**Cuvette # 3**				
	R1	**R2**	**R3**	**AvR**	**Stdev**	**R1**	**R2**	**R3**	**AvR**	**Stdev**	**R1**	**R2**	**R3**	**AvR**	**Stdev**
T12	82.8	83.2	83.2	**83.1**	**0.2**	83.7	83.8	83.7	**83.7**	**0.1**	83.9	83.7	83.8	**83.8**	**0.1**
T3	82.8	82.5	82.8	**82.7**	**0.2**	83.6	83.6	83.9	**83.7**	**0.2**	82.7	82.7	82.6	**82.7**	**0.1**
T6	83.6	83.1	83.6	**83.4**	**0.3**	83.7	83.8	83.8	**83.8**	**0.1**	82.6	82.3	82.7	**82.5**	**0.2**
T9	83.4	82.5	83.0	**83.0**	**0.5**	84.3	84.0	83.9	**84.1**	**0.2**	82.7	83.2	82.7	**82.9**	**0.3**
Tave,stdev				**83.0**	**0.1**				**83.8**	**0.1**				**83.0**	**0.1**
Cuvette Ave, stdec	**83.3**	**0.5**													

Concentration (ug/L)	**250.0**														
Power Setting	**3X**														
	Cuvette # 1					**Cuvette # 2**					**Cuvette # 3**				
	R1	**R2**	**R3**	**AvR**	**Stdev**	**R1**	**R2**	**R3**	**AvR**	**Stdev**	**R1**	**R2**	**R3**	**AvR**	**Stdev**
T12	40.9	40.9	40.9	**40.9**	**0.0**	39.5	39.5	39.5	**39.5**	**0.0**	40.5	40.6	40.4	**40.5**	**0.1**
T3	40.9	40.7	40.9	**40.8**	**0.1**	38.7	39.2	39.2	**39.0**	**0.3**	40.5	40.5	40.5	**40.5**	**0.0**
T6	40.6	40.7	40.7	**40.7**	**0.1**	39.4	39.0	38.6	**39.0**	**0.4**	40.6	40.6	40.6	**40.6**	**0.0**
T9	40.6	40.6	40.6	**40.6**	**0.0**	38.7	38.5	38.5	**38.6**	**0.1**	40.5	40.5	40.5	**40.5**	**0.0**
Tave,stdev				**40.8**	**0.1**				**39.0**	**0.2**				**40.5**	**0.1**
Cuvette Ave, stdec	**40.1**	**0.9**													

Concentration (ug/L)	100.0														
Power Setting	10x														
	Cuvette # 1					Cuvette # 2					Cuvette # 3				
	R1	R2	R3	AvR	Stdev	R1	R2	R3	AvR	Stdev	R1	R2	R3	AvR	Stdev
T12	53.5	53.4	53.3	**53.2**	**0.1**	53.3	53.5	53.6	**53.5**	**0.2**	53.7	53.7	53.7	**53.7**	**0.0**
T3	52.7	53.1	53.1	**53.1**	**0.2**	53.3	53.8	53.5	**53.5**	**0.3**	53.5	53.5	53.5	**53.5**	**0.0**
T6	53.0	52.7	52.7	**52.8**	**0.2**	54.6	54.6	54.6	**54.6**	**0.0**	53.3	53.3	53.3	**53.3**	**0.0**
T9	52.2	52.2	52.2	**52.2**	**0.0**	53.3	53.3	53.3	**53.3**	**0.0**	52.9	53.7	53.0	**53.2**	**0.4**
Tave,stdev				**52.8**	**0.1**				**53.7**	**0.1**				**53.4**	**0.2**
Cuvette Ave, stdec	**53.3**	**0.5**													

Concentration (ug/L)	0.0														
Power Setting	10x														
	Cuvette # 1					Cuvette # 2					Cuvette # 3				
	R1	R2	R3	AvR	Stdev	R1	R2	R3	AvR	Stdev	R1	R2	R3	AvR	Stdev
T12	0.0	0.0	0.0	**0.0**	**0.0**	0.0	0.0	0.0	**0.0**	**0.0**	0.0	-0.1	-0.1	**-0.1**	**0.1**
T3	0.0	0.0	0.0	**0.0**	**0.0**	0.0	0.0	0.0	**0.0**	**0.0**	0.0	0.3	0.3	**0.2**	**0.2**
T6	0.0	0.0	0.0	**0.0**	**0.0**	0.0	0.0	0.0	**0.0**	**0.0**	0.0	0.0	0.0	**0.0**	**0.0**
T9	0.0	0.0	0.0	**0.0**	**0.0**	0.0	0.0	0.0	**0.0**	**0.0**	0.0	0.1	0.0	**0.0**	**0.1**
Tave,stdev				**0.0**	**0.0**				**0.0**	**0.0**				**0.0**	**0.1**
Cuvette Ave, stdec	0.0	0.0													

Concentration (ug/L)	P	AvR	CAvR	Mave	Stdev	Cdev	Mdev
500	3X	83.3	116.3	11.6	0.5	0.7	**0.1**
250	3X	40.1	54.2	5.4	0.9	1.3	**0.1**
100	10X	53.3	15.5	1.5	0.5	0.1	**0.0**
0	10X	0.0	0.0	0.0	0.0	0.0	**0.0**